Earth magnetotail current sheet: observations vs. models

Anton Artemyev

IGPP/UCLA

in collaborations with: Vassilis Angelopoulos (IGPP/UCLA), San Lu (IGPP/UCLA), Anatoliy Petrukovich (IKI/RAS), Andrei Runov (IGPP/UCLA), Ivan Vasko (SSL/UCB), Lev Zelenyi (IKI/RAS).

Location and plasma parameters

Plasma β – ratio of plasma and magnetic field pressures

Mach number M – ratio of plasma bulk velocity and magnetosonic speed

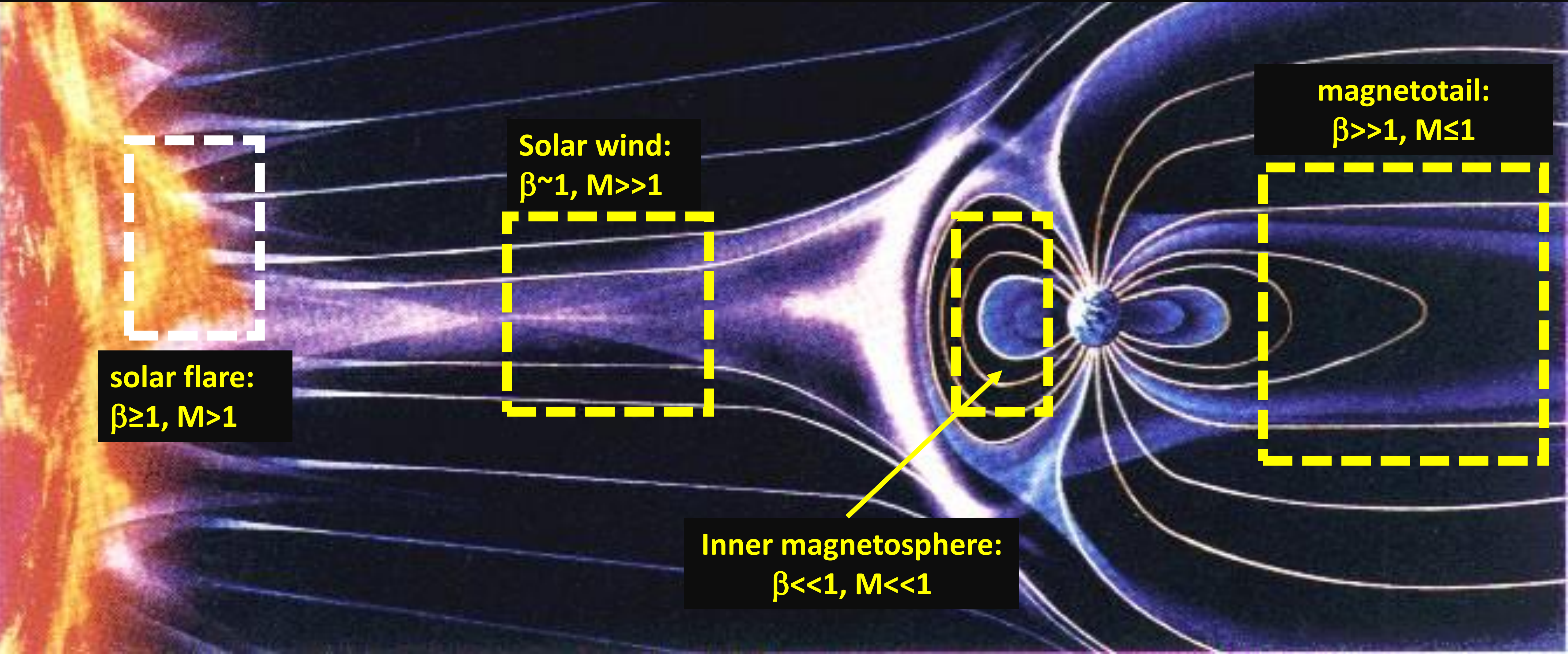

The simplest current sheet configuration

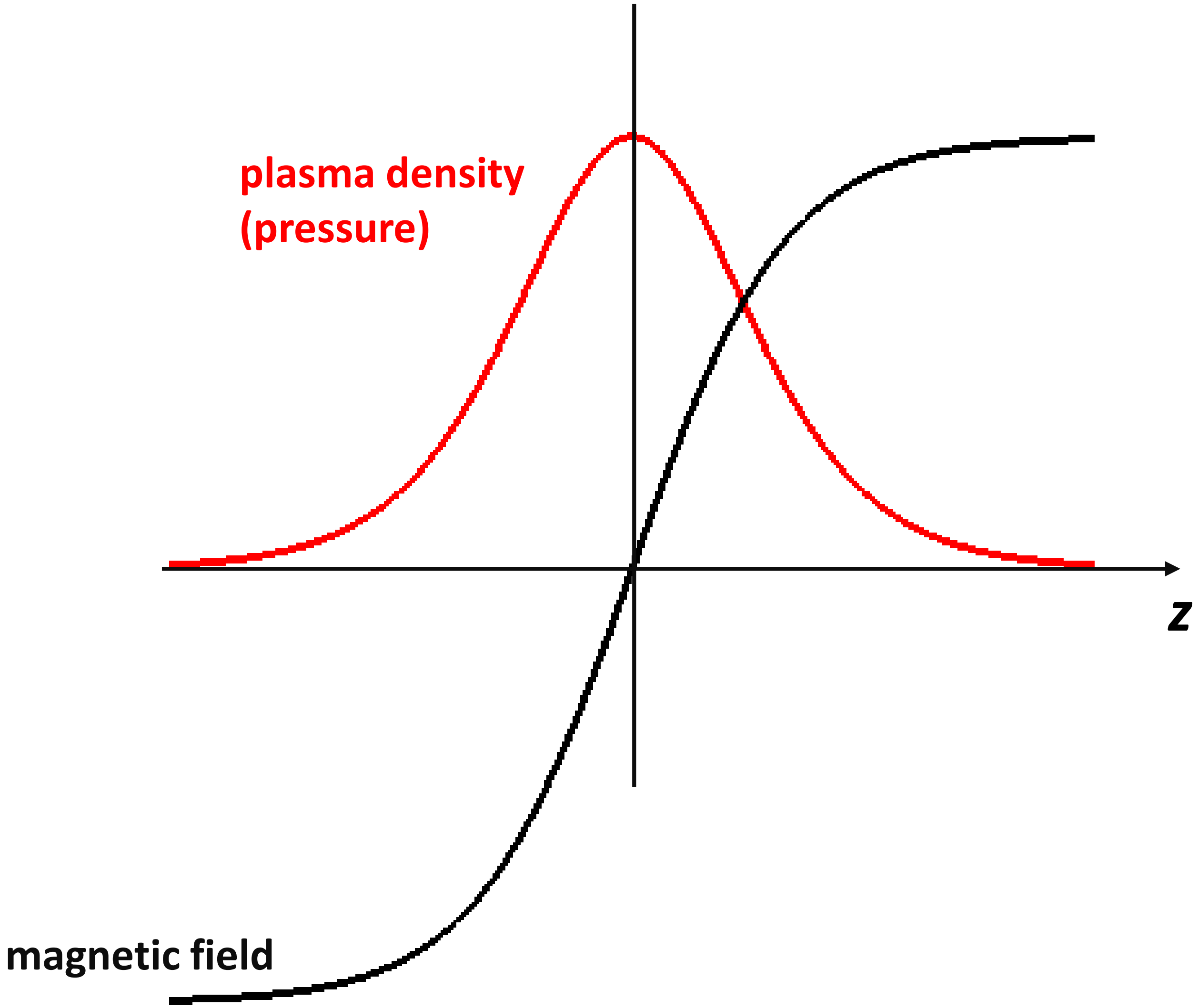

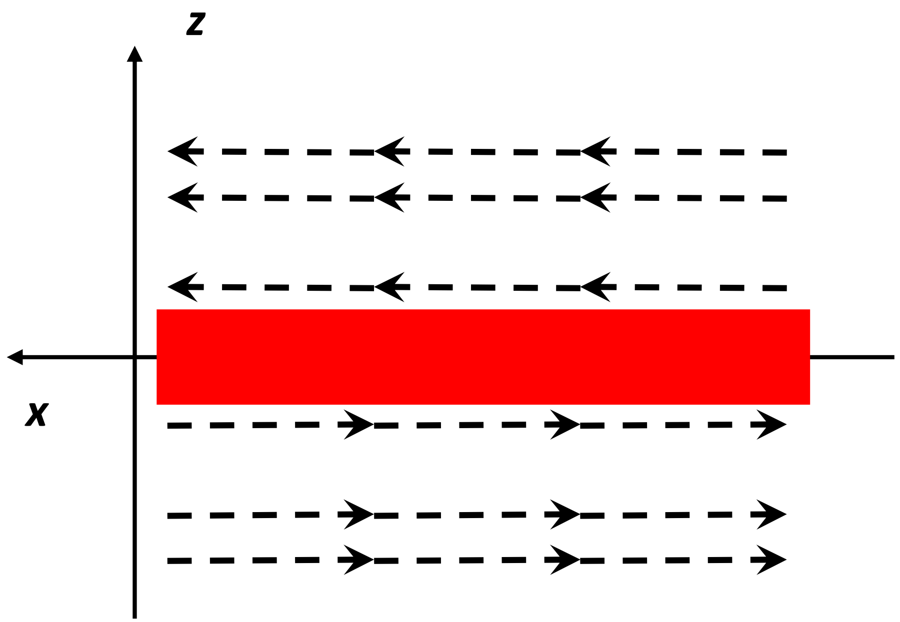

Diamagnetic plasma current

$$j_y = -c \frac{T}{B_x} \frac{dn}{dz}$$

Self-consistent fields and plasma motion

Stationary Maxwell equations

$$\nabla \times \mathbf{B} = \frac{4\pi}{c}\mathbf{j} + \frac{1}{c}\frac{\partial \mathbf{E}}{\partial t}$$

$$\nabla \cdot \mathbf{E} = 4\pi\rho$$

$$\nabla \times \mathbf{E} = -\frac{1}{c}\frac{\partial \mathbf{B}}{\partial t}$$

$$\nabla \cdot \mathbf{B} = 0$$

+

Currents and charged density

$$\mathbf{j} = \sum_{\pm}\int \mathbf{v} q_{\pm} f_{\pm}(\mathbf{v}, r)\, d\mathbf{v}$$

$$\rho = \sum_{\pm}\int q_{\pm} f_{\pm}(\mathbf{v}, r)\, d\mathbf{v}$$

ions (+) and electrons (-)

+

Vlasov equation

$$\frac{\partial f_{\pm}}{\partial t} + \mathbf{v}\frac{\partial f_{\pm}}{\partial \mathbf{r}} + \frac{\mathbf{F}_{\pm}}{m_{\pm}}\frac{\partial f_{\pm}}{\partial \mathbf{v}} = 0$$

Lorentz force

$$\mathbf{F}_{\pm} = q_{\pm}\mathbf{E} + \frac{1}{c}[\mathbf{v} \times \mathbf{B}]$$

Nonlinear equations for electromagnetic fields

An example of solutions: 1D Harris CS

An example of solutions: 2D Fadeev CS

An example of solutions: 2D Kan CS

Magnetic field lines (black) and plasma pressure (color)

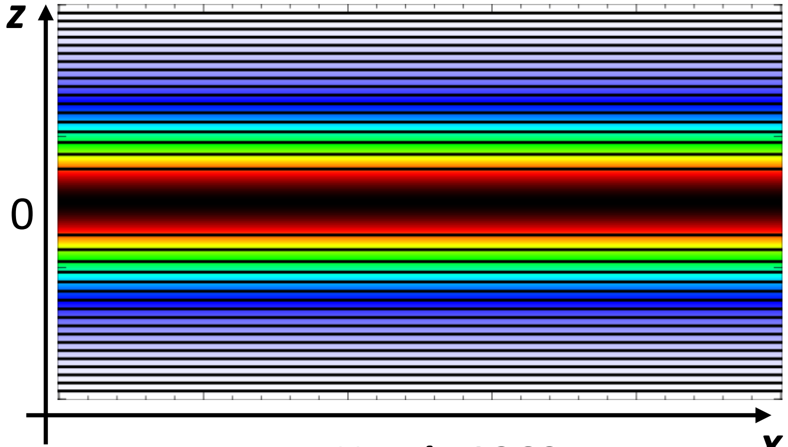

Harris 1962

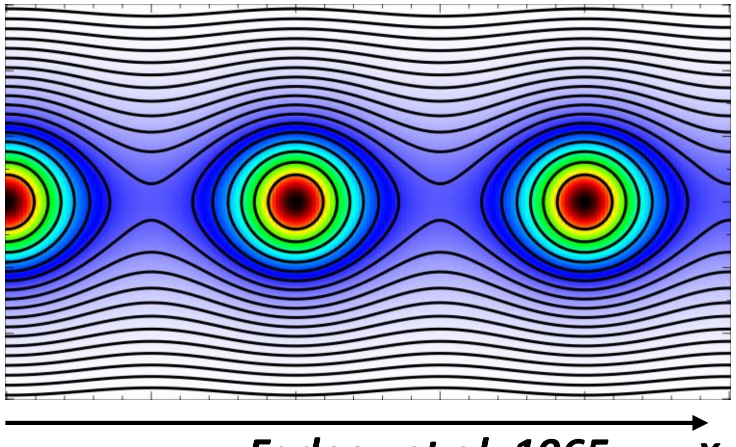

Fadeev et al. 1965

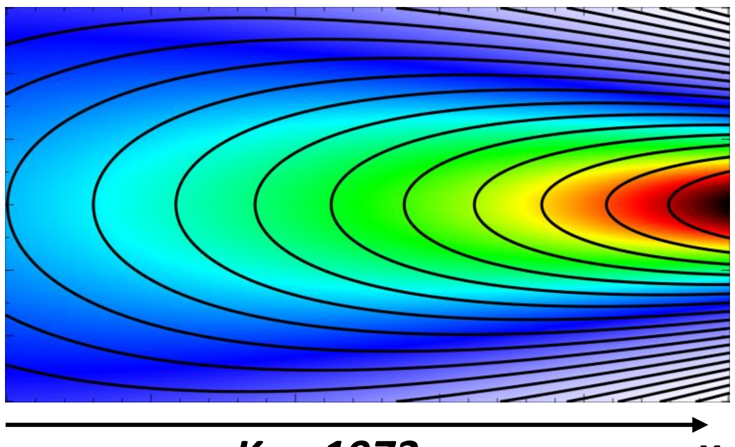

Kan 1973

Spacecraft missions and available datasets

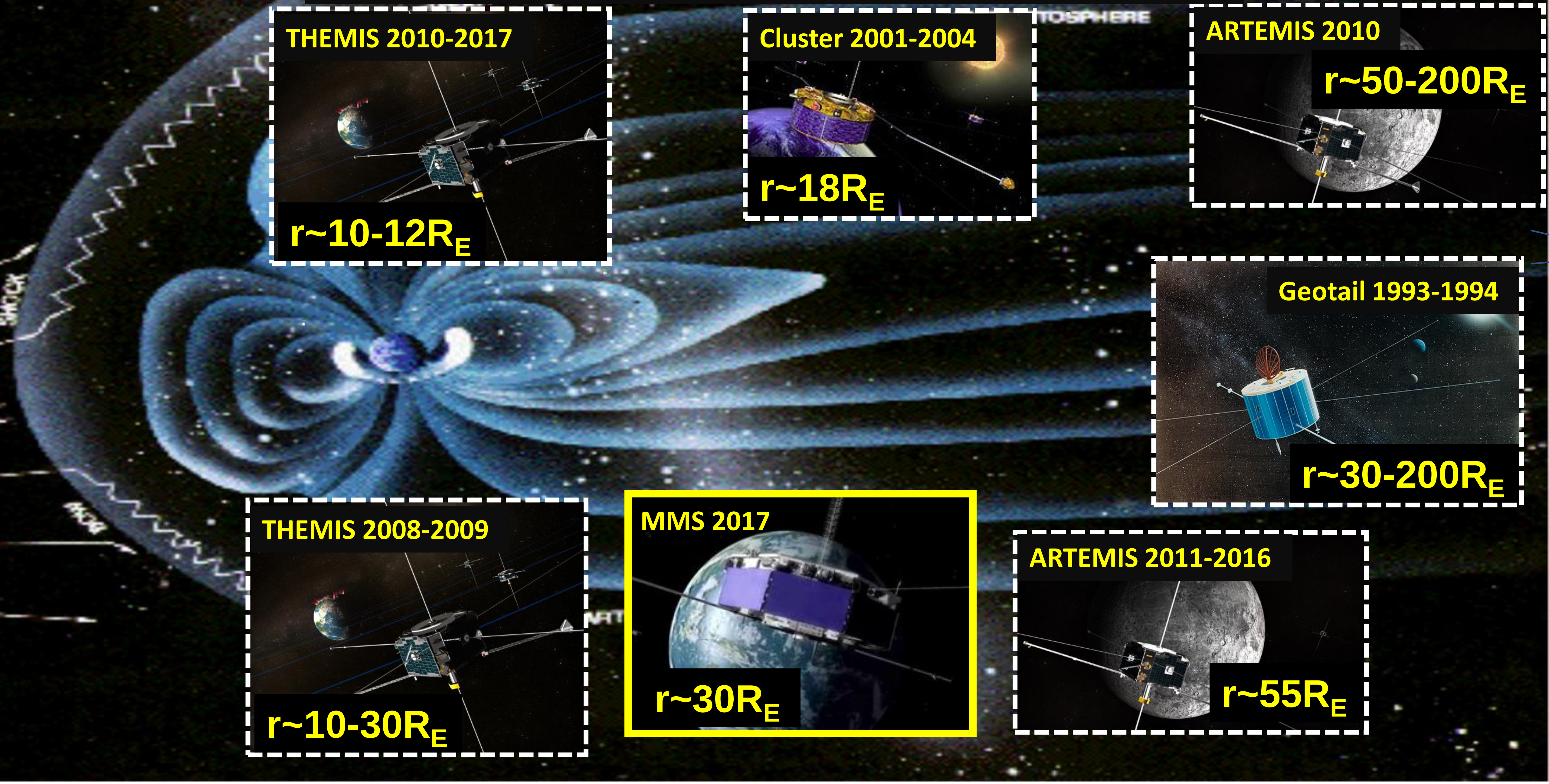

Outline:

- **Current sheet structure**: *distributions of currents and plasma, embedding, main gradients*
- **Current carriers in the magnetotail**: *electron and ion contributions*
- **Pressure balance**: *role of plasma anisotropy/nongyrotropy in current sheet balancing*
- **Electric fields**: *mechanisms of generation, typical amplitudes*
- **Current sheet thinning**: *pre-reconnection conditions in the magnetotail*

Current sheet structure: thin current sheets

Typical CS thickness is about 2000 km << R_E

Runov et al., 2006; Petrukovich et al. 2015; Vasko et al. 2015; Artemyev et al., 2016.

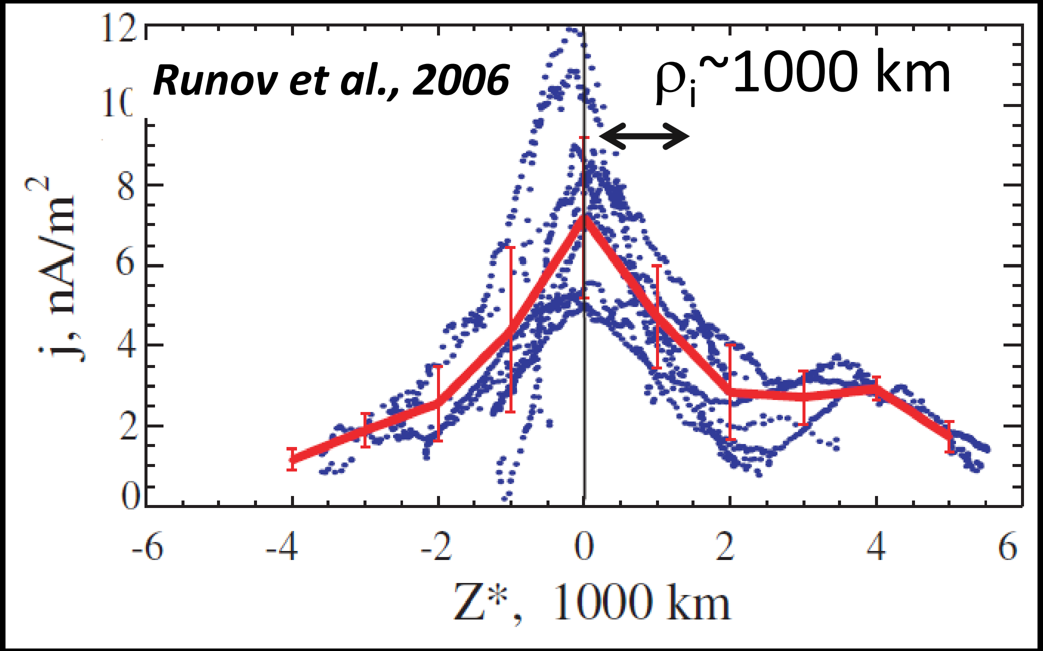

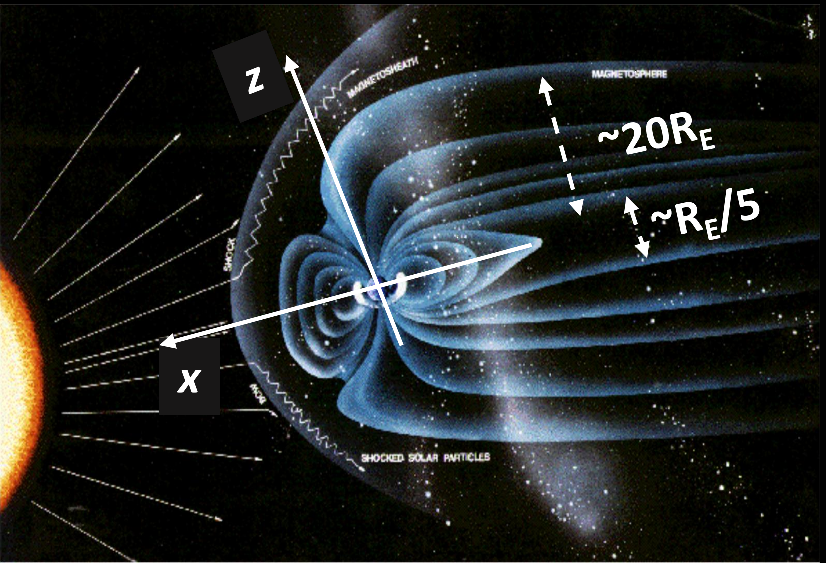

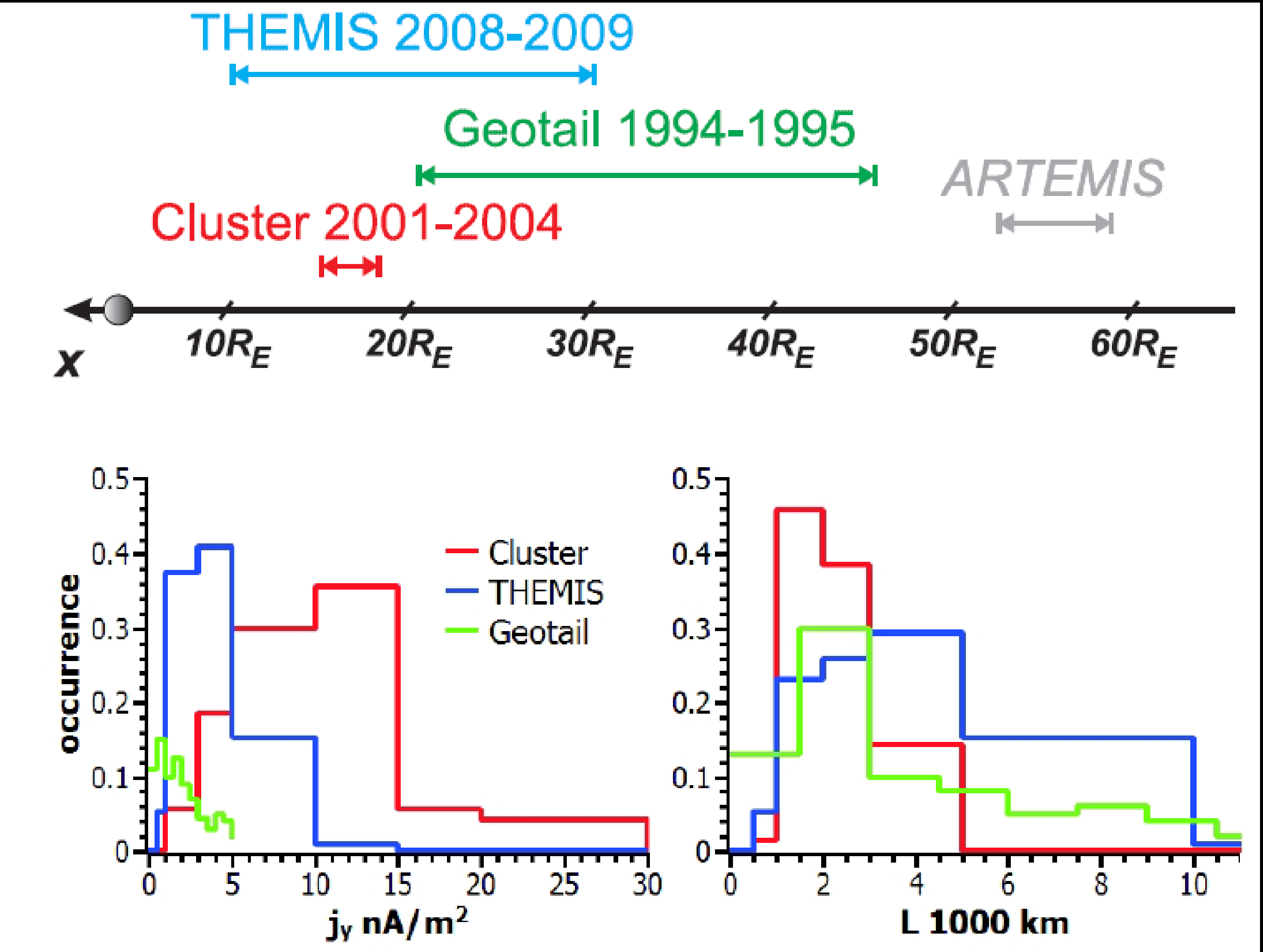

Current sheet structure: embedding

Absence of significant density variation along z-axis

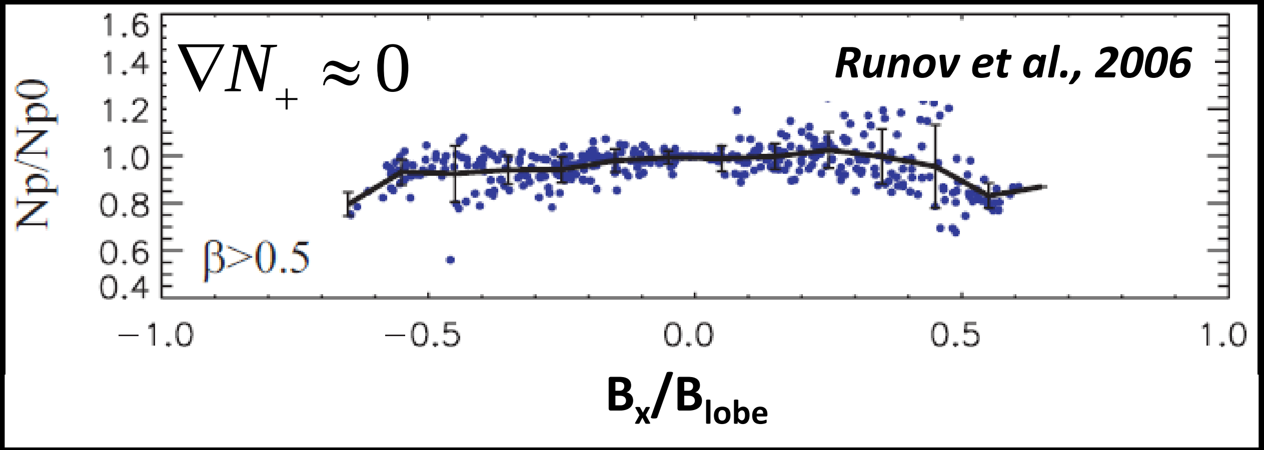

Magnetic field as a distance along z-axis: $B_x/B_{lobe} \sim z/L_{CS}$

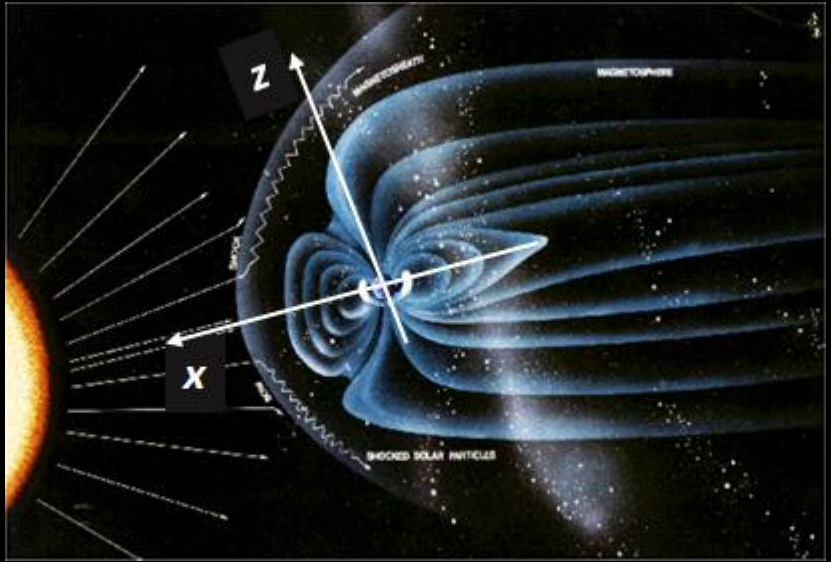

Electron and ion pressure gradients are mainly supported by temperature gradients

$$\nabla P_- \approx N_- \nabla T_-, \quad \nabla P_+ \approx N_+ \nabla T_+$$

Petrukovich et al., 2015

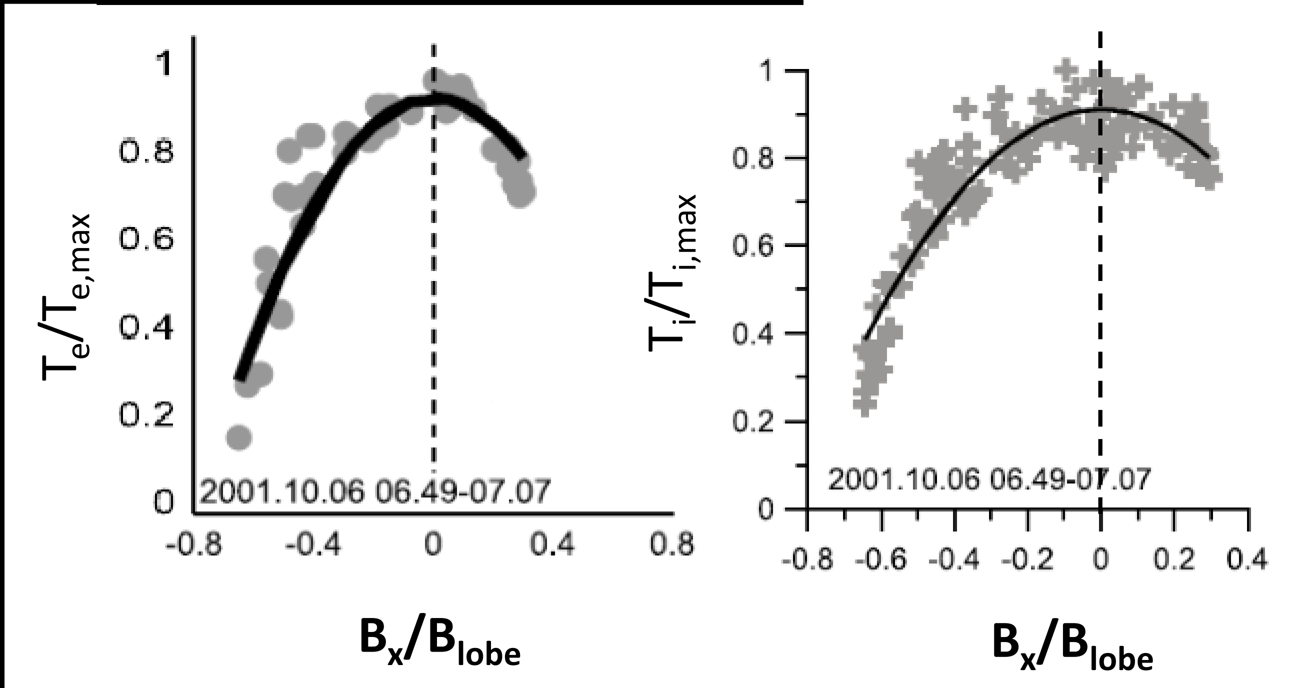

CS structure: observations vs. simple kinetic models

Harris CS model with 10-20% of cold background plasm

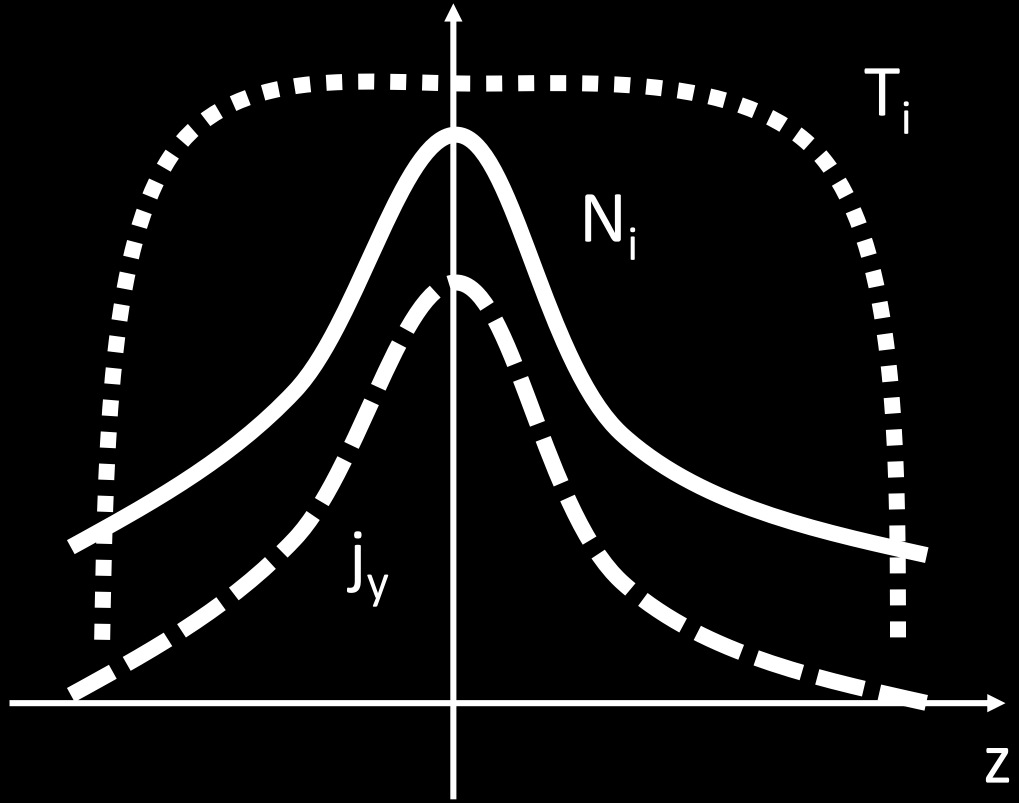

- Lobes are filled by rarified cold plasma, but CS boundaries are hot due to uniform temperature.
- Plasma density profile is very close to the current density profile

Observed current sheets

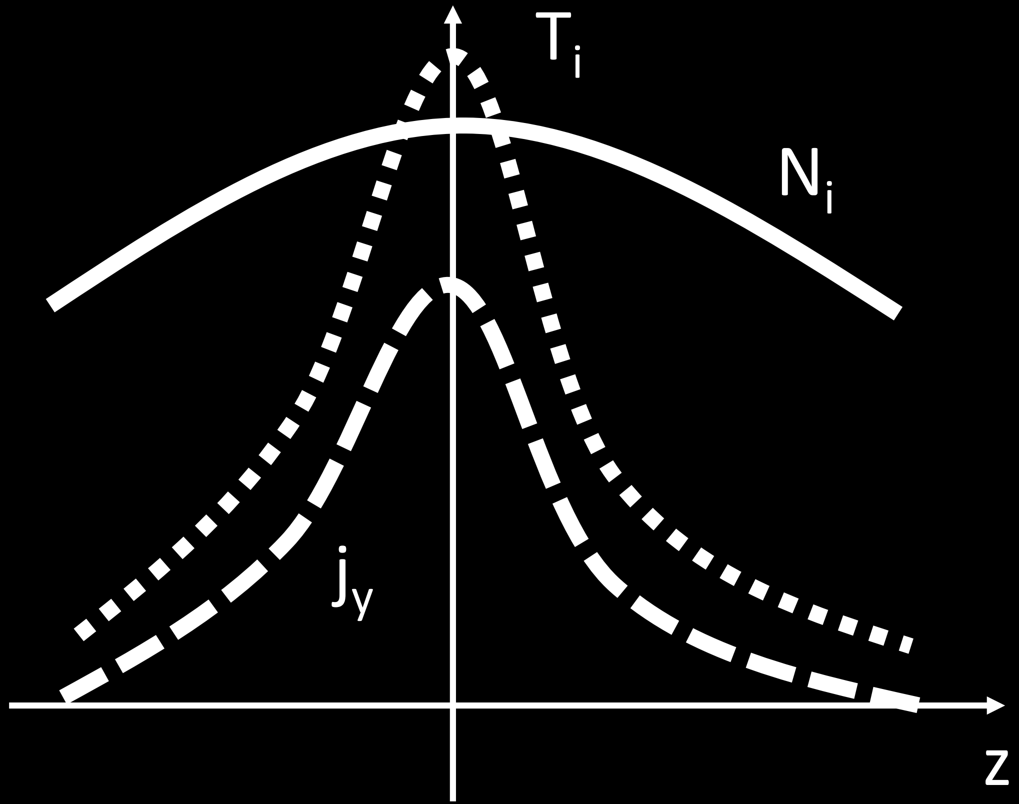

- Lobes and CS boundaries are filled by dense cold plasma.
- Current density profile is embedded into plasma density profile

CS structure: what model can reproduce CS structure?

Kinetic models do not describe strong temperature gradients for 2D (x,z) CS configurations, but can reproduce embedded current density profile

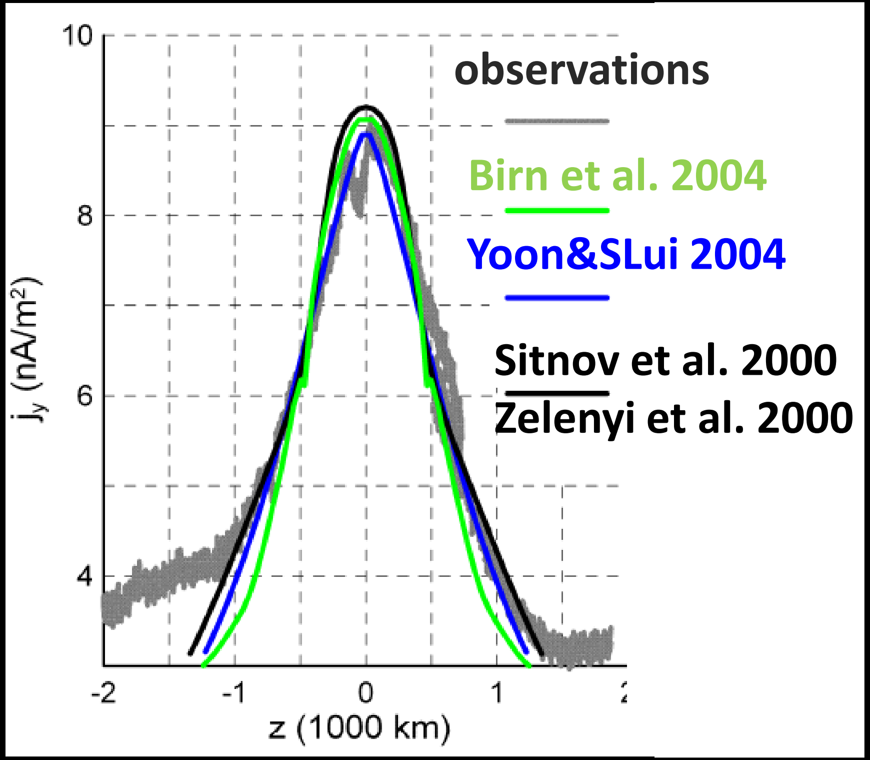

see also Schindler & Birn 2002; Sitnov et al., 2006; Zelenyi et al.

Hybrid simulations (MHD electrons + kinetic ions) are flexible enough to reproduce both embedding and temperature distributions.

see also Lin et al. 2015, Lu et al. 2016

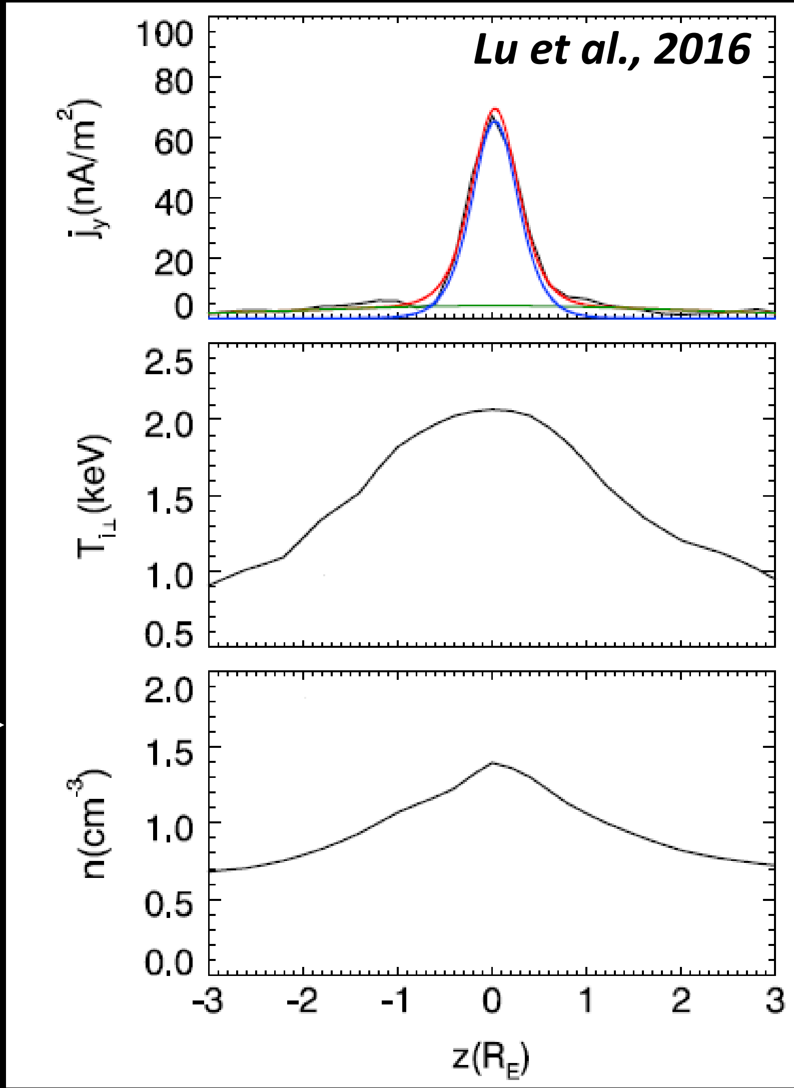

Current carriers: absence of ion currents

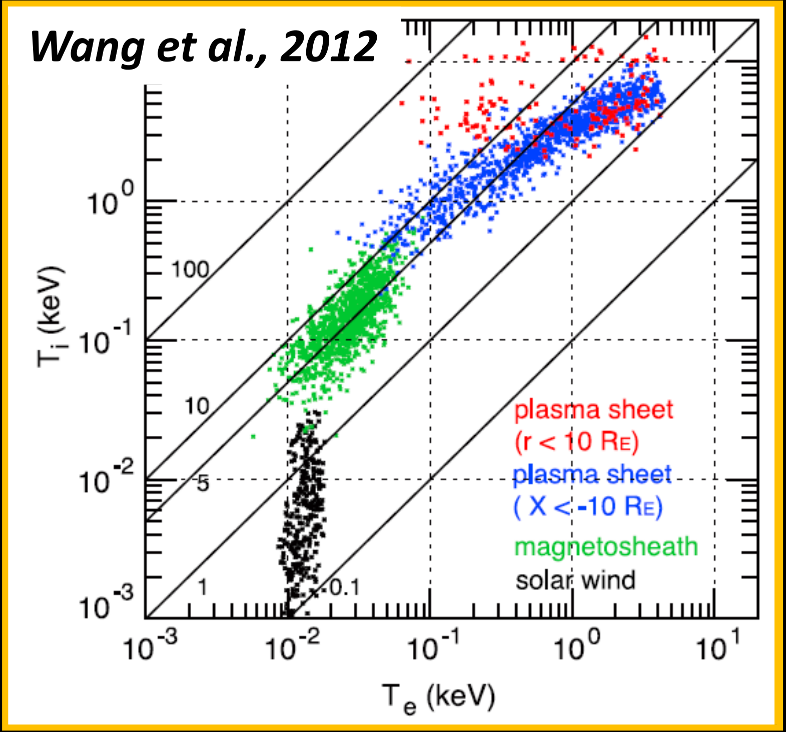

$T_i >> T_e$ thus we would expect to observe strong ion diamagnetic currents.

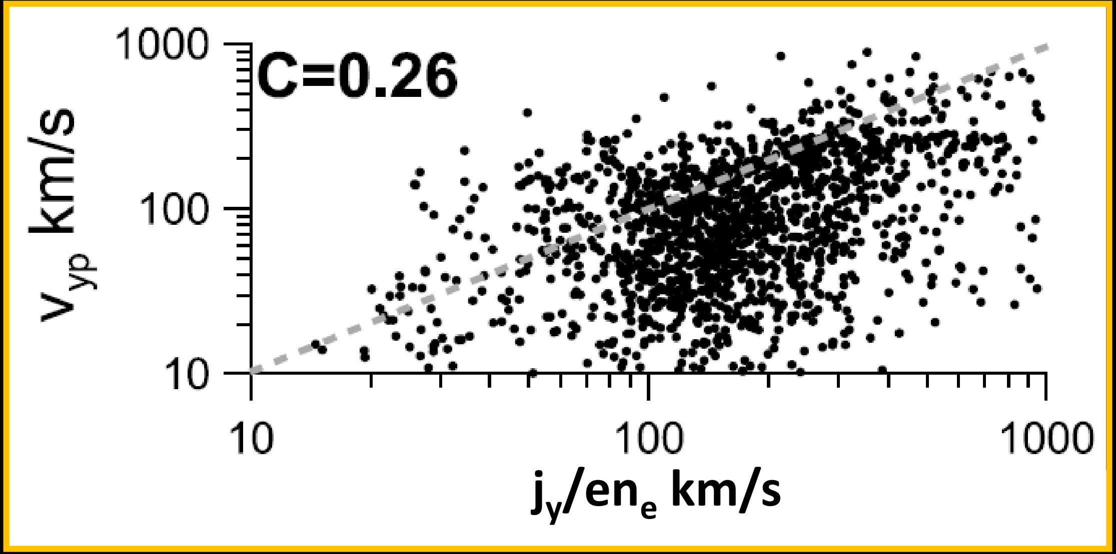

Artemyev et al., 2015

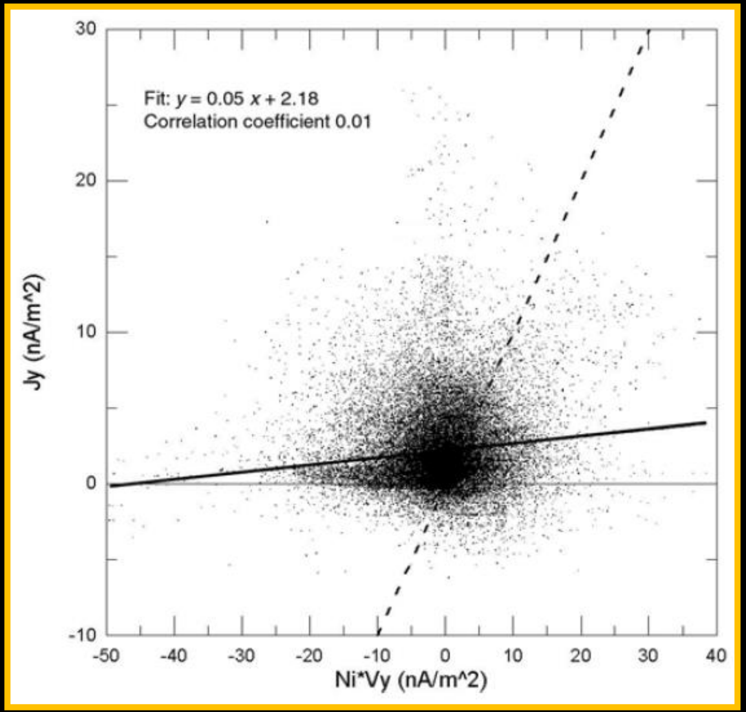

Comparison of B-gradient currents and ion currents for subset of CSs

Israelevich et al., 2008

Examples of ion current observations in CSs

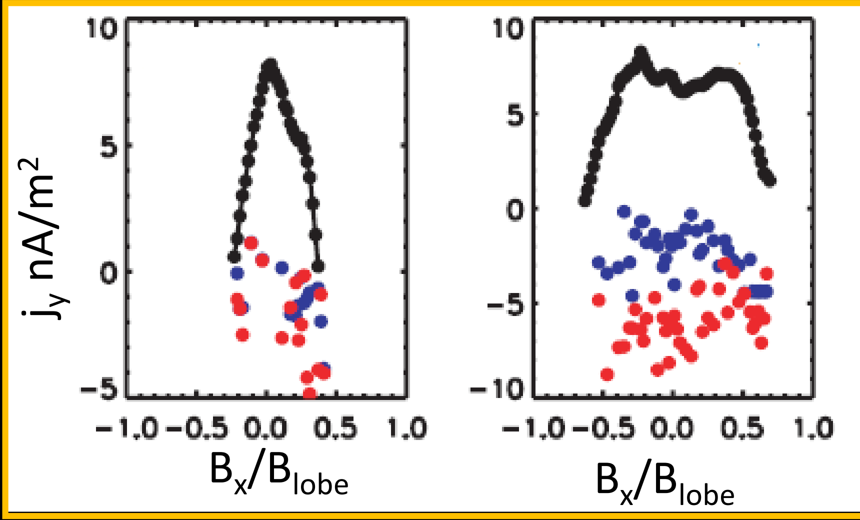

currents from B-gradients

Ion currents C4

Ion currents C1

Runov et al., 2006

Current carriers: unexpectedly strong electron currents

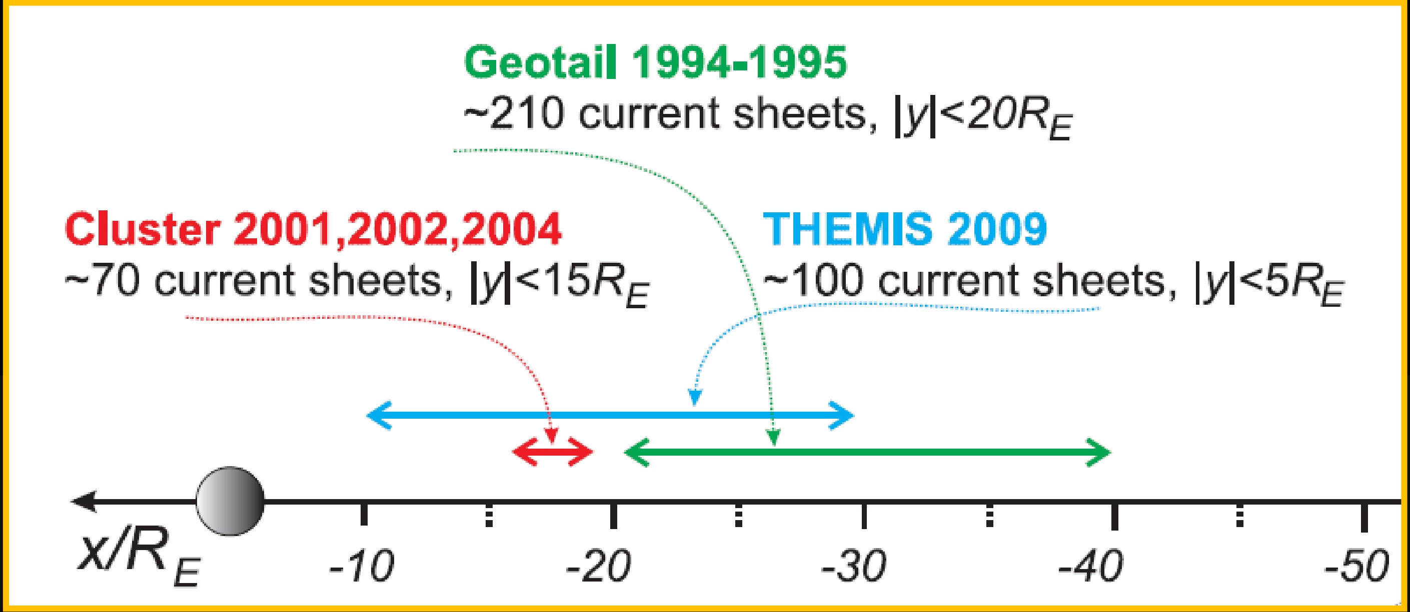

Three data sets show the same effect of strong electron currents and weak ion currents. Plasma (ion + electron) currents are close to B-gradient currents derived from multispacecraft measurements (Cluster) or from CS oscillations/flapping (Geotail, THEMIS).

see also Vasko et al., 2015; Petrukovich et al., 2015; Artemyev et al., 2016

Geotail

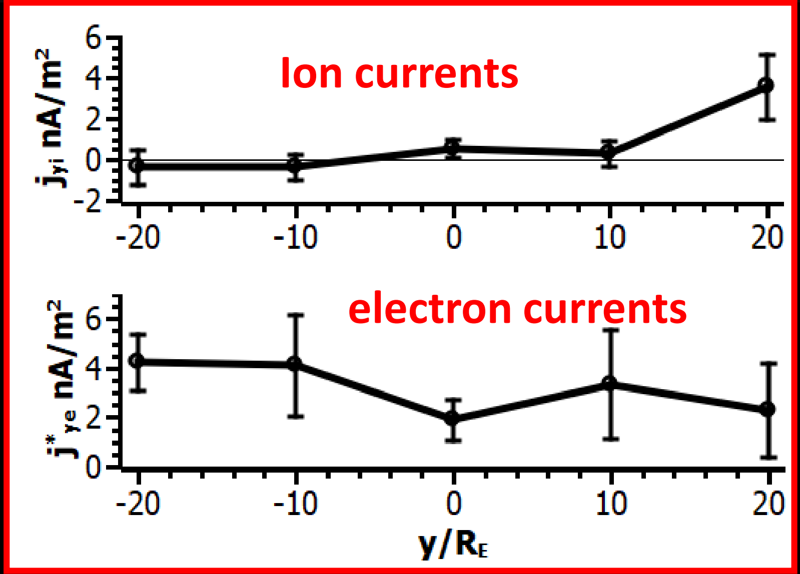

Cluster

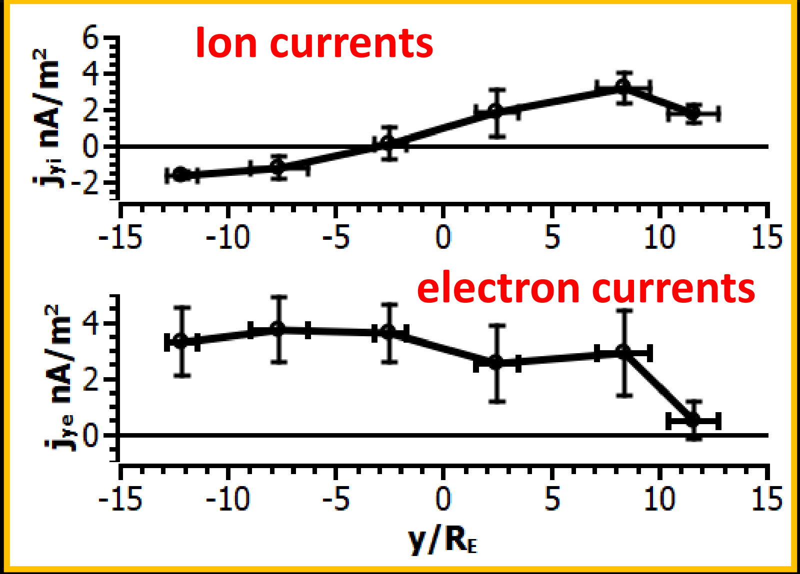

THEMIS

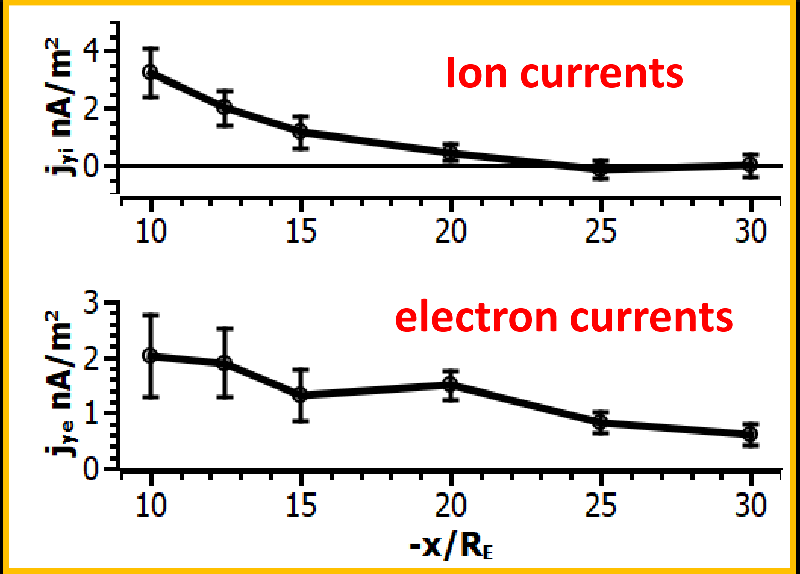

Current carriers: observations vs. models

Conservation of total plasma momentum in volume $\mathcal{V}$

ion (+) and electron (-) currents

rate of total plasma momentum change

$$\frac{d}{dt}\int_{\mathcal{V}} n\mathbf{v}_{\pm}d\mathcal{V} = \frac{m_+}{m_+ + m_-}\left(\mathbf{M} \pm \frac{1}{e}\frac{m_-}{m_\pm}\frac{d\mathbf{J}}{dt}\right)$$

total current

factor ~m-/m_+<<1 for ions. Thus, if the total momentum is conserved (**M** = 0), the change of the total current **J** is mainly due to change of the electron flow $n\mathbf{v}_-$

Hesse et al., 1998

Kinetic thin CS formation

CS thinning and intensification of j_y~enΔv current density in PIC simulation

Increase of electron flow

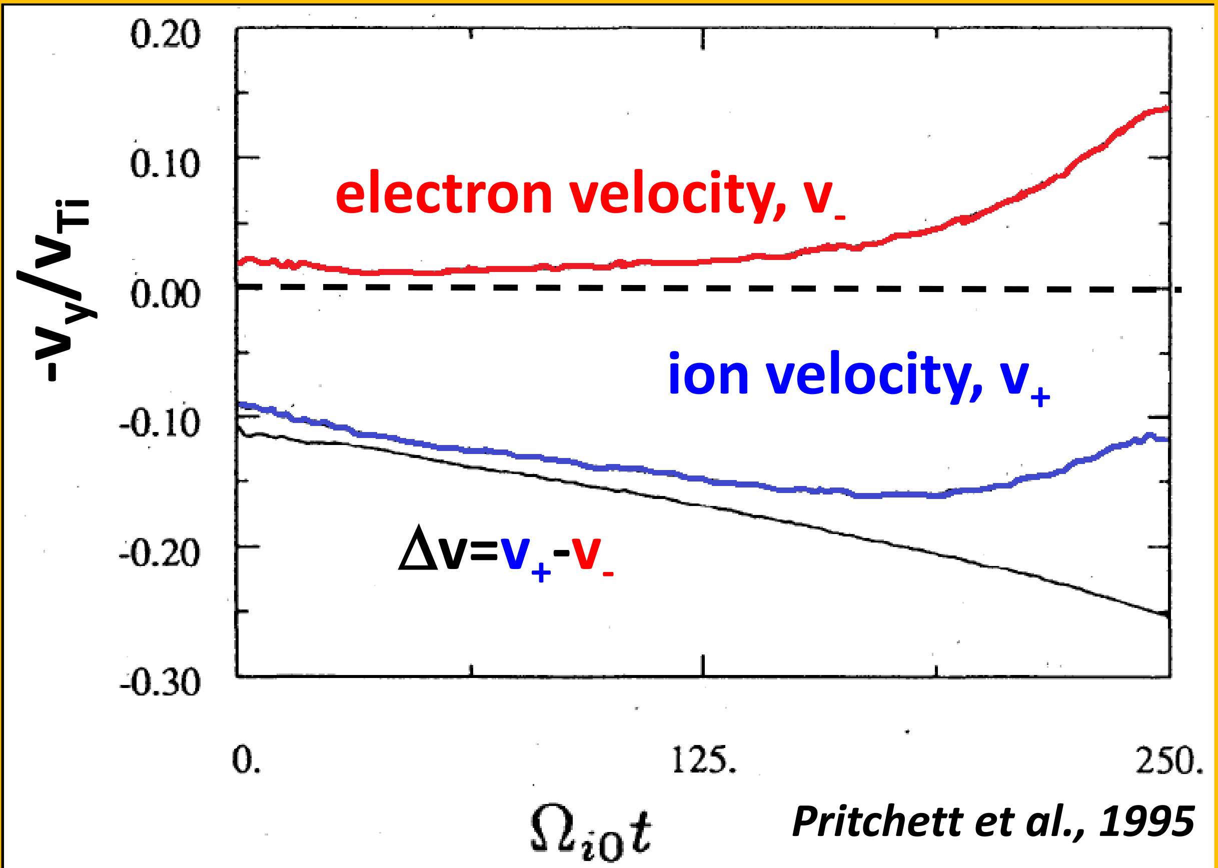

Pritchett et al., 1995

Pressure balance: expected gradients

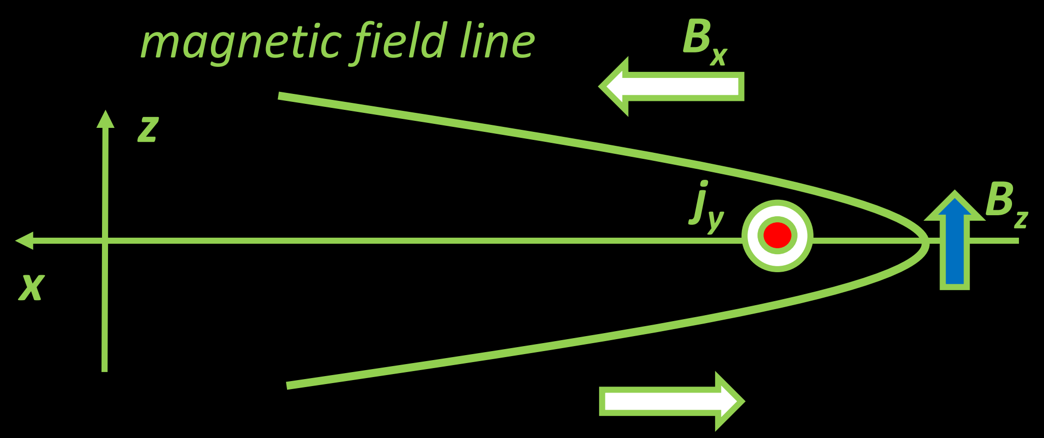

B_{lobe} distribution along the tail

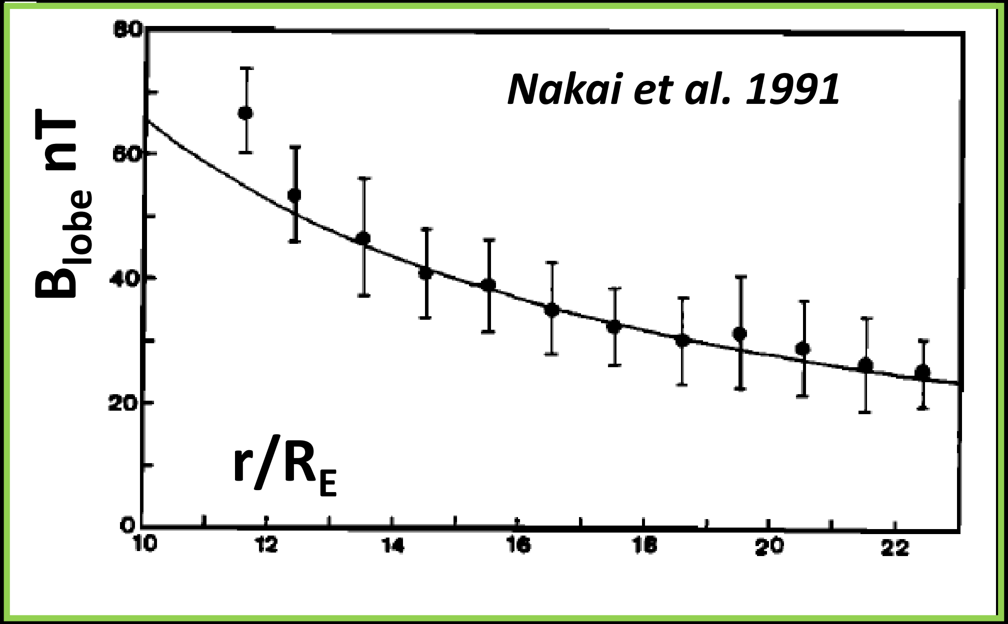

static pressure balance

$$\sum_{\pm} \nabla \hat{p}_{+} = \frac{1}{c}[\mathbf{j} \times \mathbf{B}]$$

Isotropic plasma pressure $p_p = p_+ + p_-$

Balance along z

Balance along x

$$\frac{\partial}{\partial z}\left(p_p + \frac{B_x^2}{8\pi}\right) \approx 0, \quad \frac{\partial p_p}{\partial x} \approx \frac{1}{c} B_z j_y$$

Current density magnitude is defined by the lobe magnetic field distribution

$$j_y \approx \frac{c}{4\pi} \frac{B_{lobe}}{B_z} \frac{\partial B_{lobe}}{\partial x}, \quad B_{lobe} = \sqrt{8\pi p_P}$$

Pressure balance: statistical observations

Nakai et al. 1991;Shukhtina et al. 2004

$$B_{lobe} \approx 20\mathrm{nT} \cdot \left(r / 25R_E \right)^{-0.8}$$

upper limit for j_y at $r \sim 18R_E$

$$j_y < 2\ \mathrm{nA/m^2}$$

observed j_y are much larger than expected values

THEMIS measurements

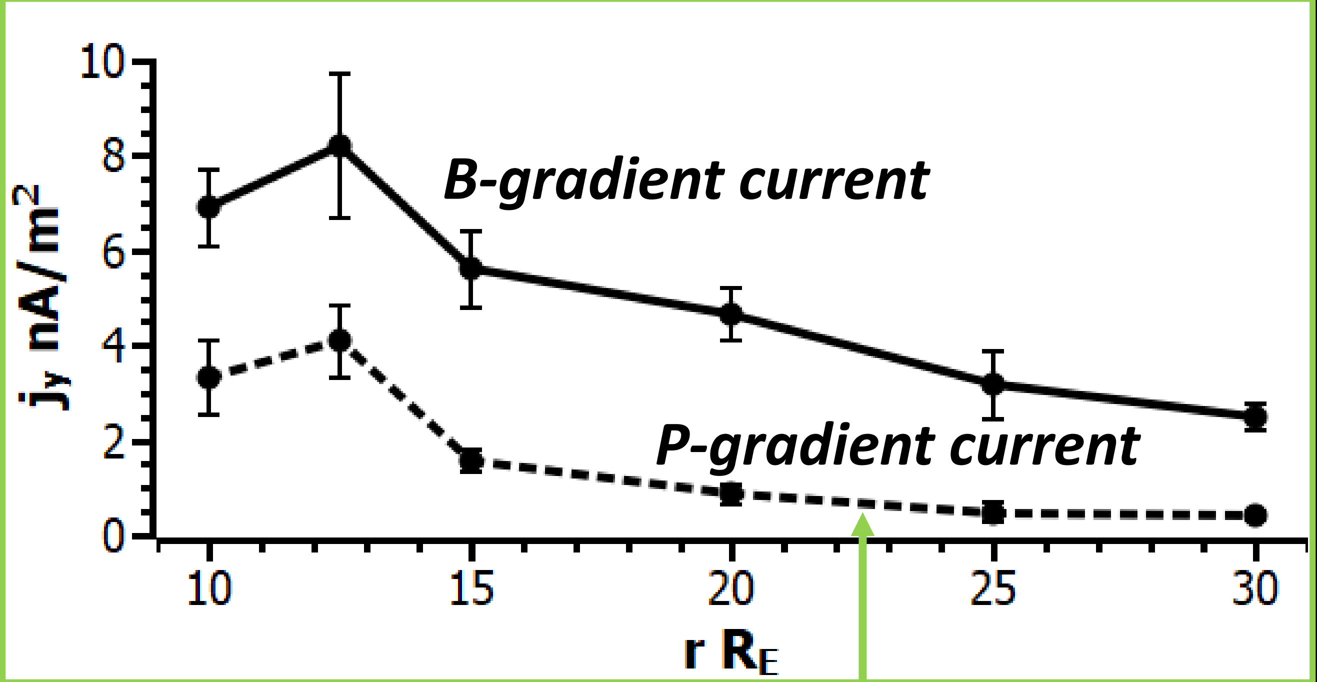

$$j_y(x) \approx \frac{c}{4\pi} \frac{B_{lobe}}{B_z} \frac{\partial B_{lobe}}{\partial x}$$

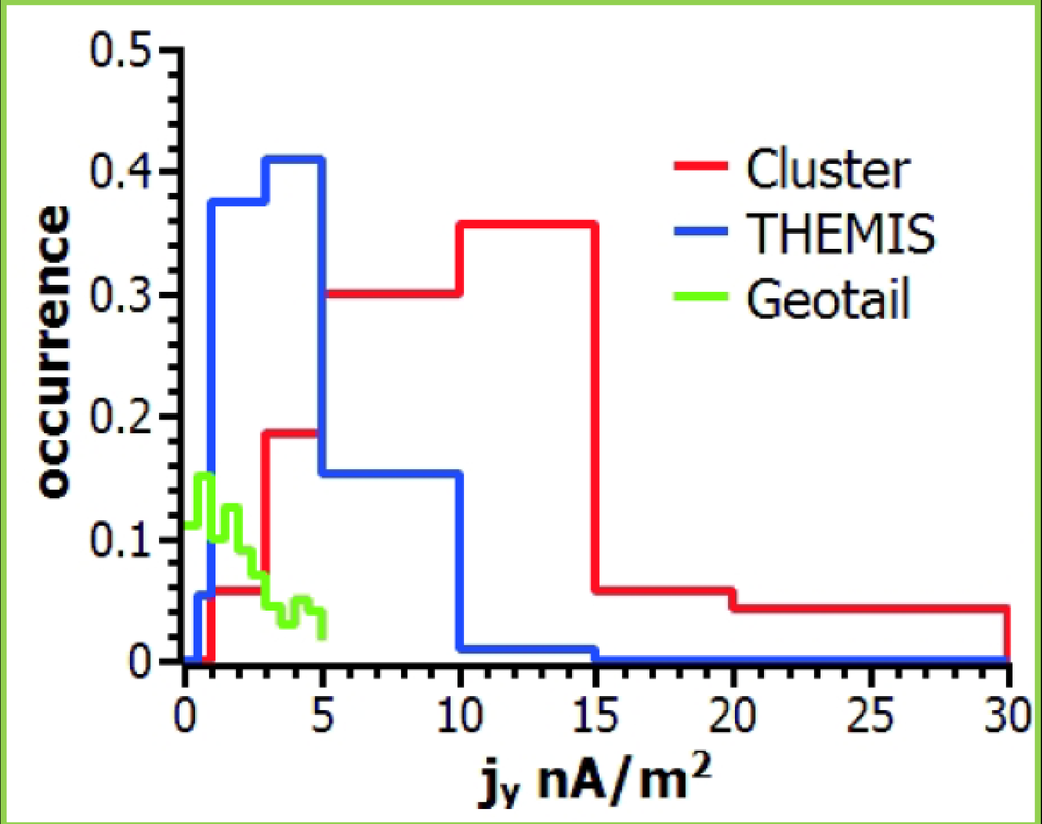

Pressure balance: electron anisotropy

curvature force

$$\nabla p_p + \frac{\Lambda_e}{4\pi}\frac{\left[\mathbf{B}\times(\mathbf{B}\nabla)\mathbf{B}\right]}{B} = \frac{\left[\mathbf{j}\times\mathbf{B}\right]}{c}$$

$$p_p = p_i + p_{e\perp}, \quad \Lambda_e = \frac{4\pi(p_{e\|} - p_{e\perp})}{B^2}$$

at the equatorial plane (B_x=0)

$$j_y \approx \frac{c}{4\pi}\frac{1}{1-\Lambda_e}\frac{B_{lobe}}{B_z}\frac{\partial B_{lobe}}{\partial x}$$

Field-aligned electron anisotropy helps balance current sheet. For Λ_e=1 the entire current density generated by curvature electron drifts (d/dx=0)

THEMIS observations

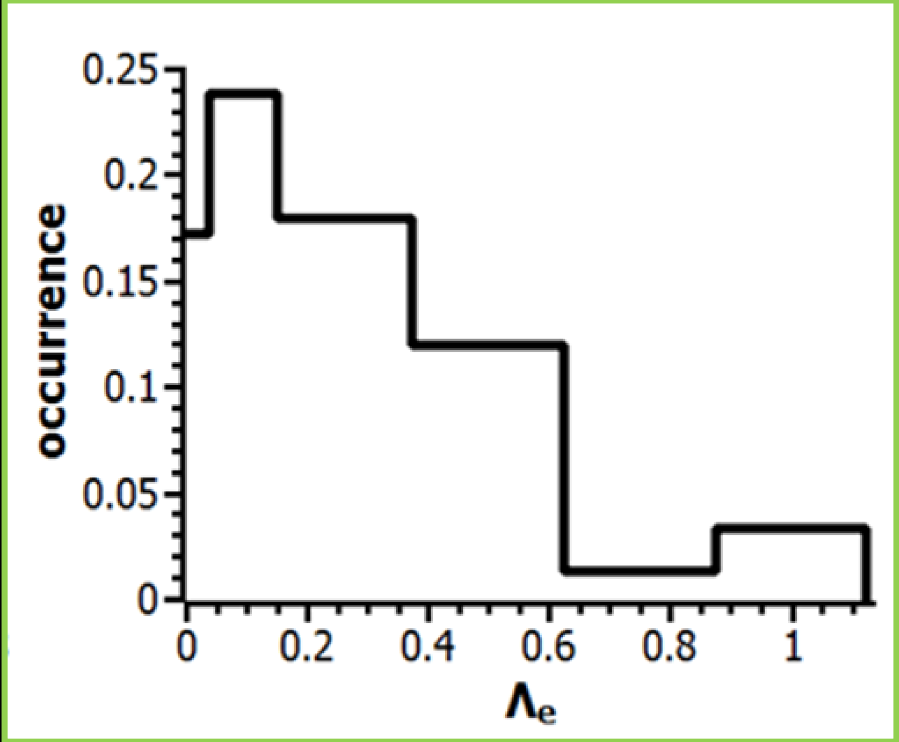

There is a significant population of CSs with almost isotropic electrons

Pressure balance: observations vs. models

Ion nongyrotropy can balance CS

$$\frac{\partial p_{xz}}{\partial z} = \frac{1}{c} j_y B_z$$

PIC simulation of thin CS

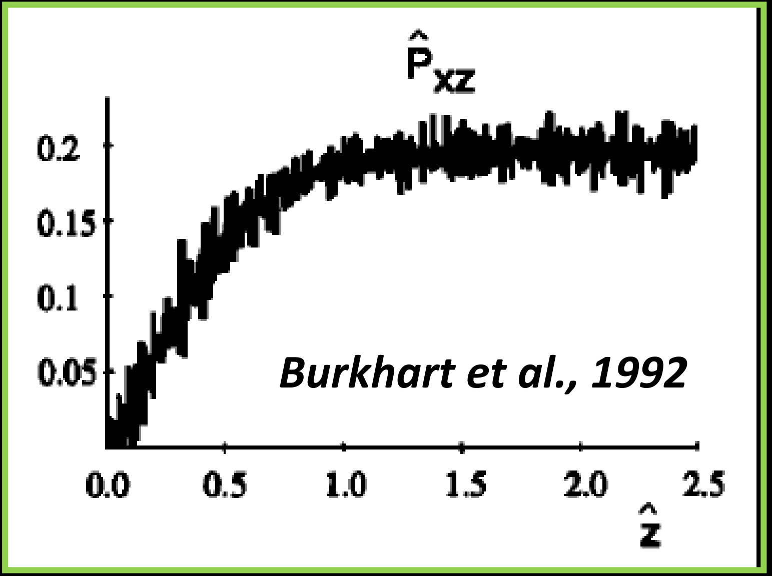

see also Eastwood 1972; Pritchett and Coroniti 1992; Ashour-Abdalla et al., 1994;

distribution function of ions supporting $p_{xz} \neq 0$

Observations

models

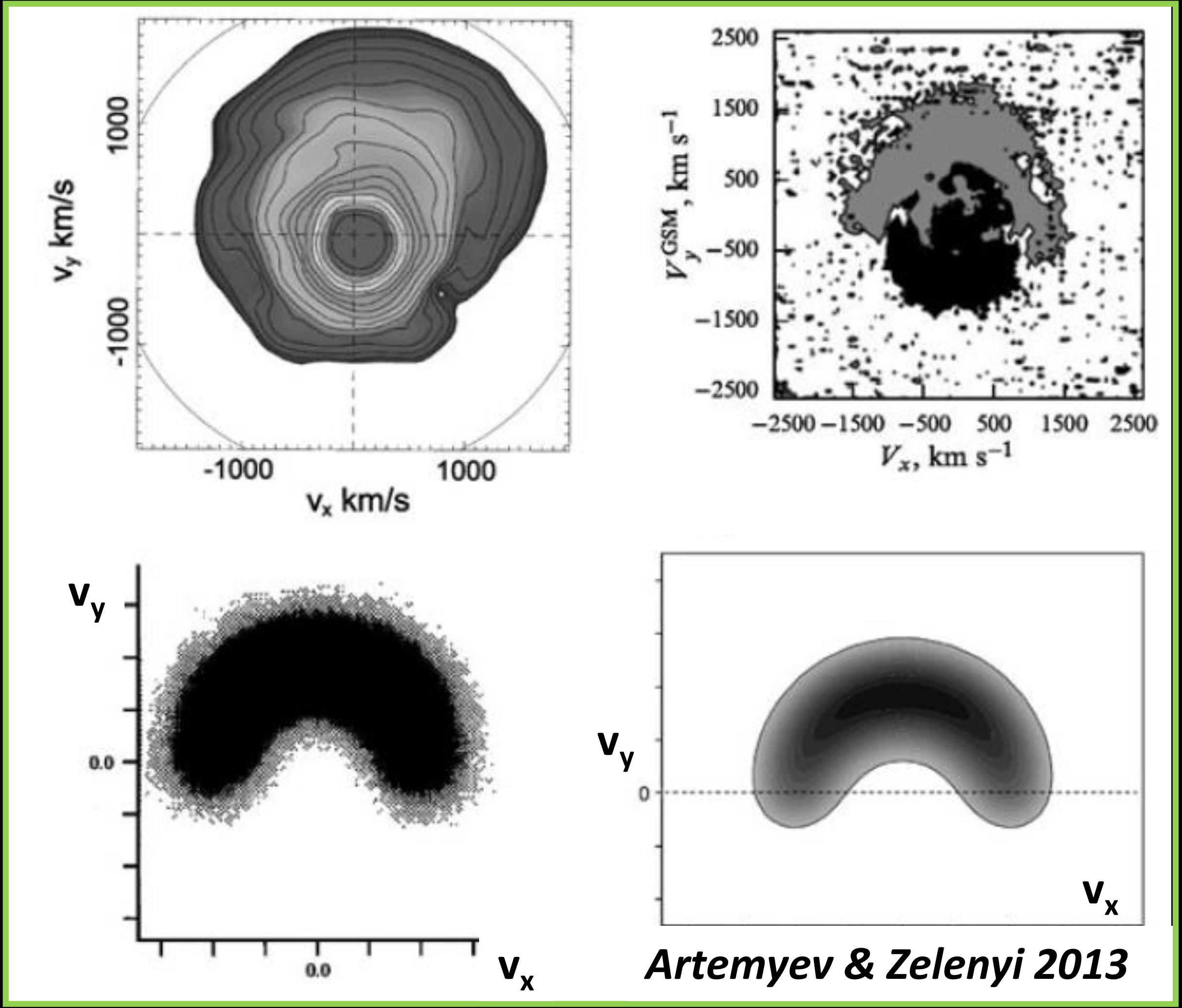

see also Sitnov et al., 2004; Zhou et al., 2009; Zelenyi et al. 2011

Electric fields: Hall field in thin CS

Dominance of electron currents requires strong electric fields E_x, E_z

$$v_{E\times B} = c\frac{[\mathbf{E}\times\mathbf{B}]_y}{B^2} = c\frac{E_zB_x - E_xB_z}{B^2}$$

$$E_z \sim \frac{v_{E\times B}}{c}B_x \sim \frac{j_y}{qn_+c}B_x \sim 1\,\mathrm{mV/m}$$

$$E_x \sim E_z\frac{B_z}{B_{lobe}} < 0.1\,\mathrm{mV/m}$$

Cluster & THEMIS can provide reliable electric field measurements only in CS (x,y) plane. Therefore, observed electric fields can be estimated only for strongly titled CS with z<->y

Cluster crossing of very intense CS

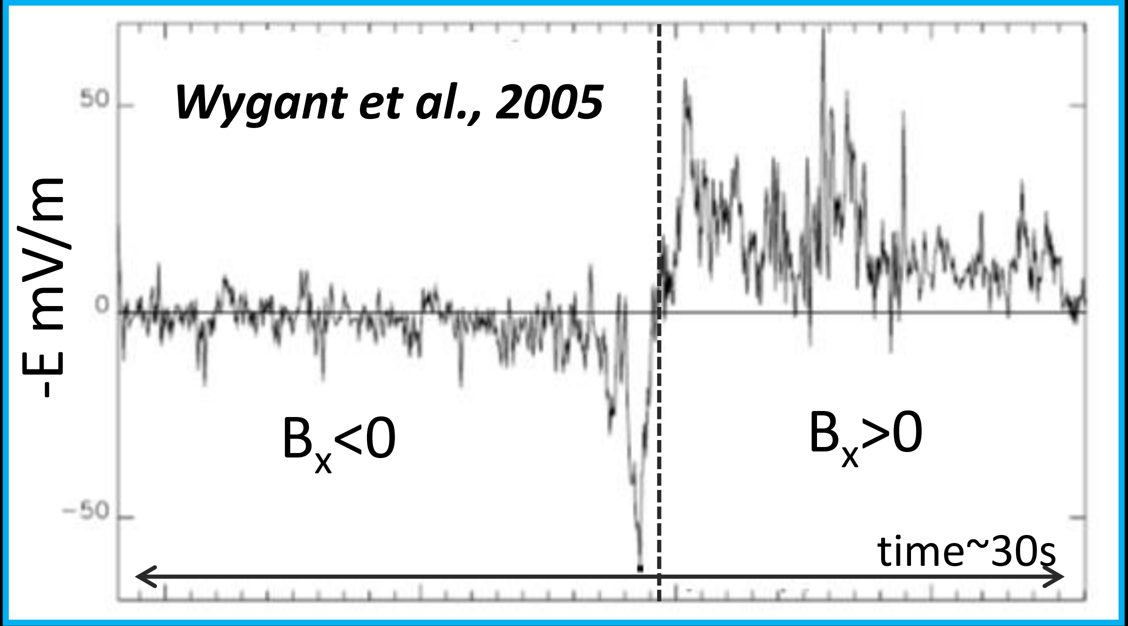

Statistics of quiet CSs

Vasko et al., 2014

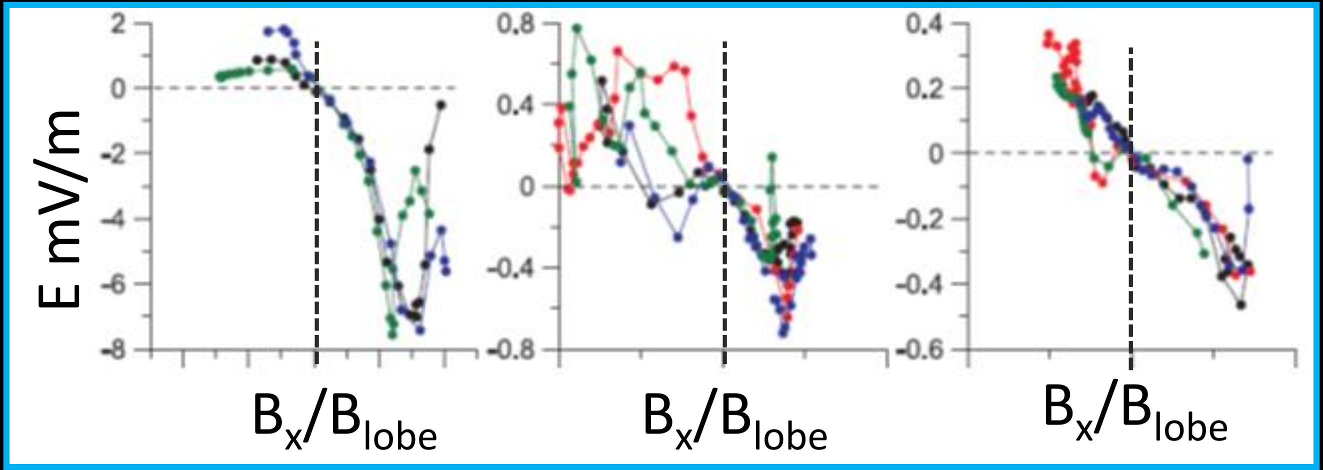

Electric fields: field-aligned field

Electron stress balance along magnetic filed lines

$$en_e E_{\|} = -\nabla_{\|} p_{\|e} + \frac{p_{\|e} - p_{\perp e}}{B^2} \frac{\mathbf{B}(\mathbf{B}\nabla)B}{B}$$

$$\alpha_e = \left\langle \frac{p_{\|e}}{p_{\perp e}} \right\rangle \approx 1.1 - 1.2$$

$n_e \approx$ const

$$eE_{\|} = -T_{\perp e} \nabla_{\|} \ln \left(\frac{T_{e\perp}^{\alpha_e}}{B^{\alpha_e - 1}} \right)$$

$$E_{\|} < 0.1\,\mathrm{mV/m}$$

Cluster statistics

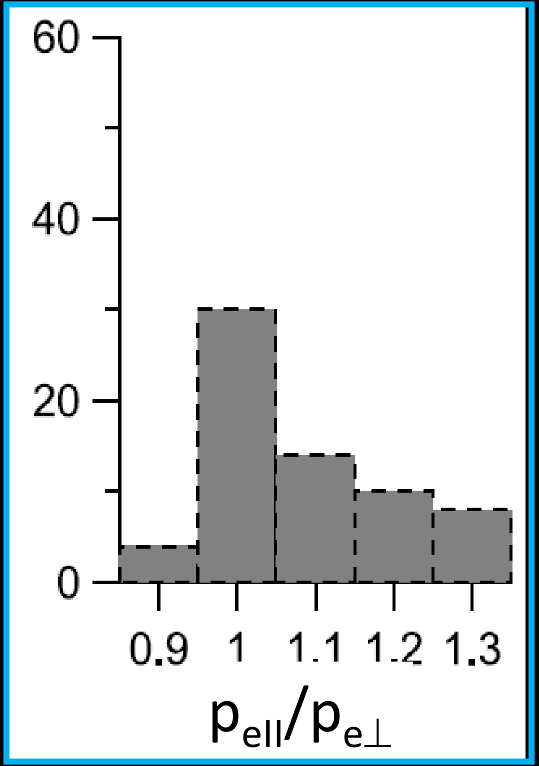

THEMIS statistics

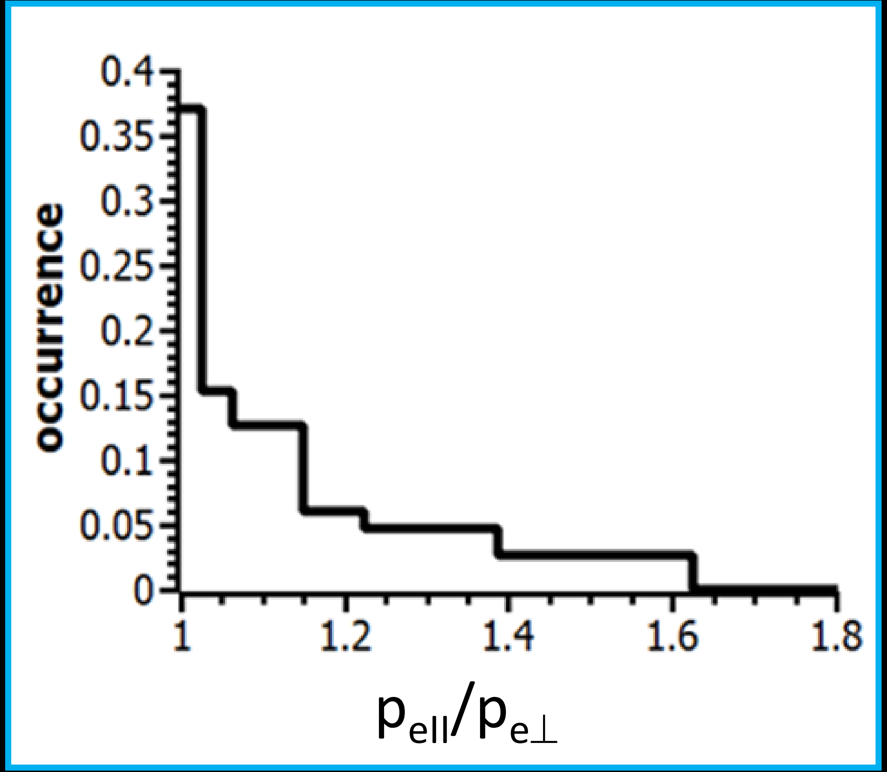

Electric fields: observations vs. models

Transverse electric field (Ex, Ez)

PIC simulations

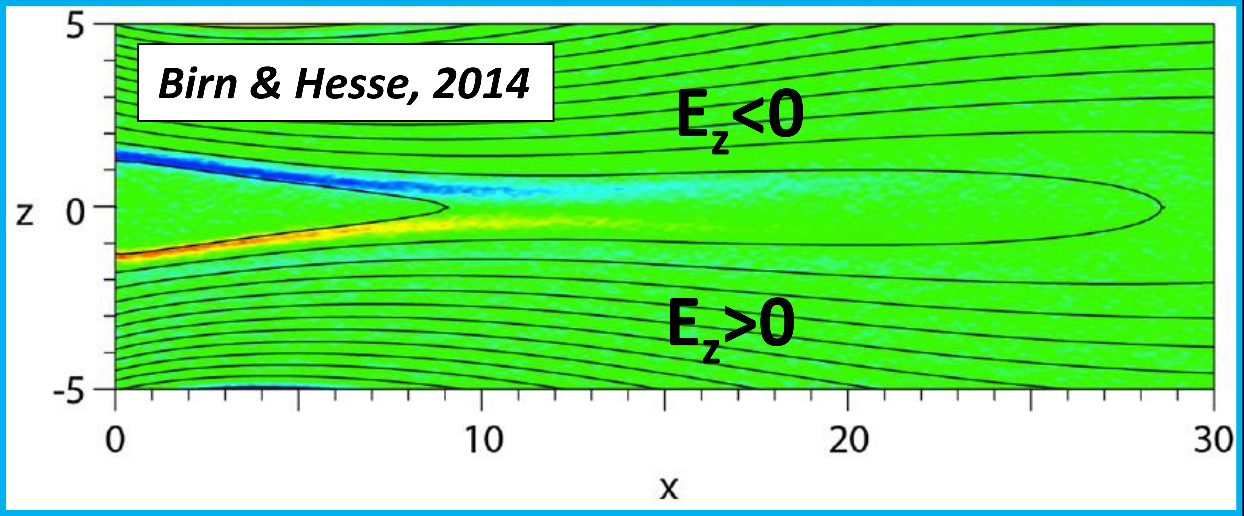

Field-aligned electric field (E_{II})

PIC simulations

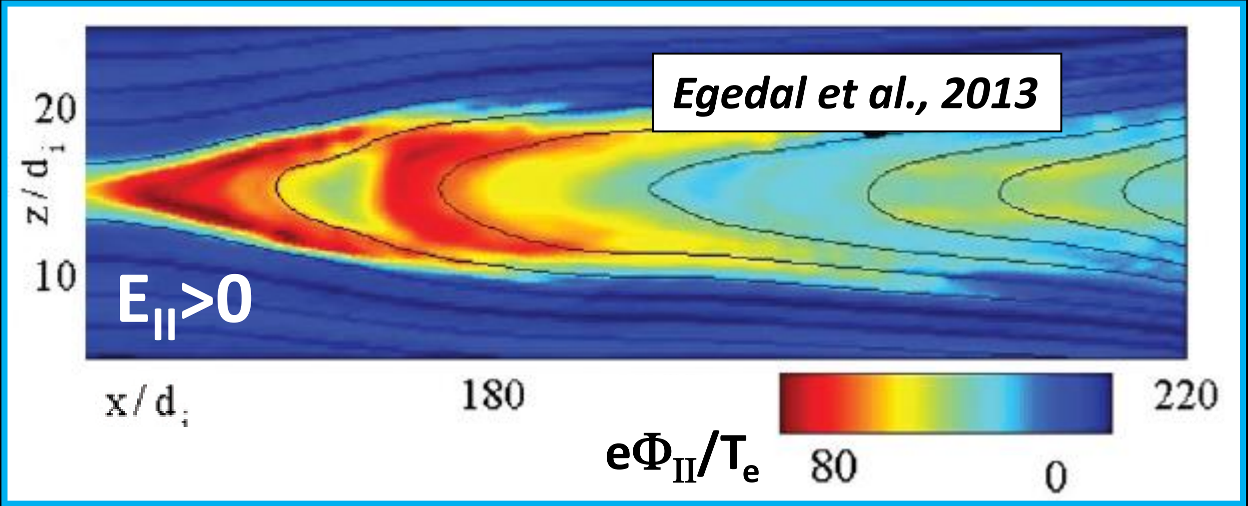

Hybrid simulations

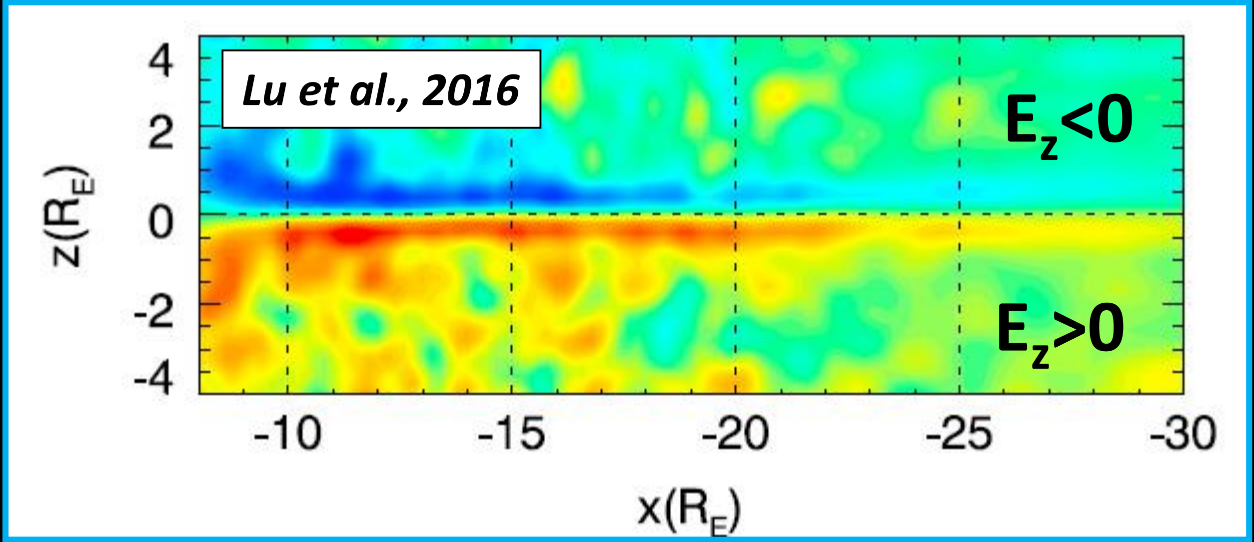

Analytical CS model

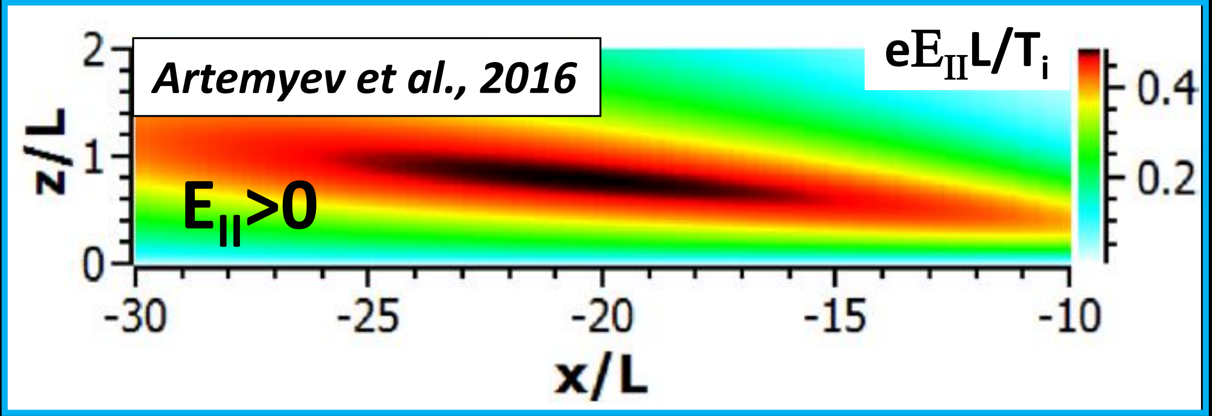

see also Pritchett 2005; Zelenyi et al. 2011;Schindler et al. 2012;

Current sheet dynamics: thinning

McPherron et al. 1972

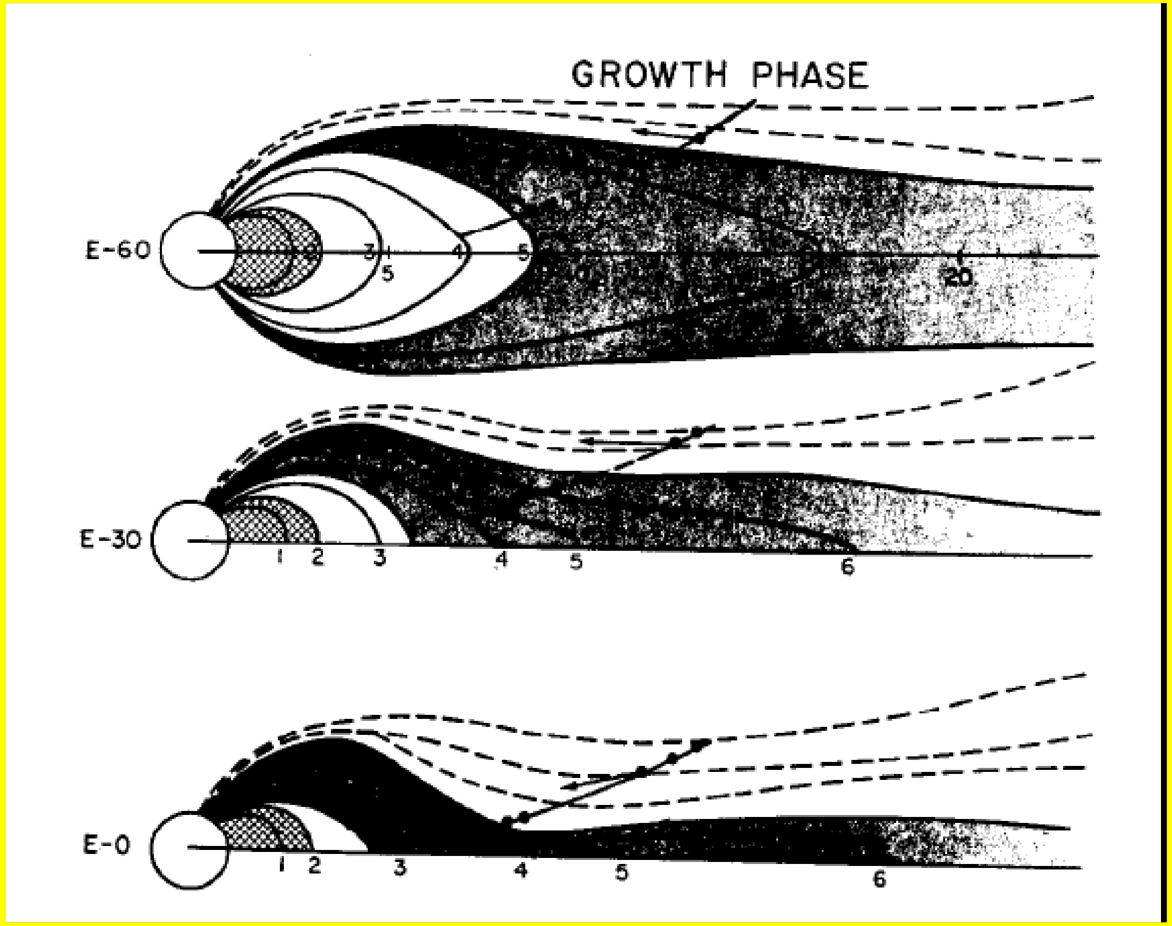

An example of thinning CS observed by THEMIS at x~-12R_E

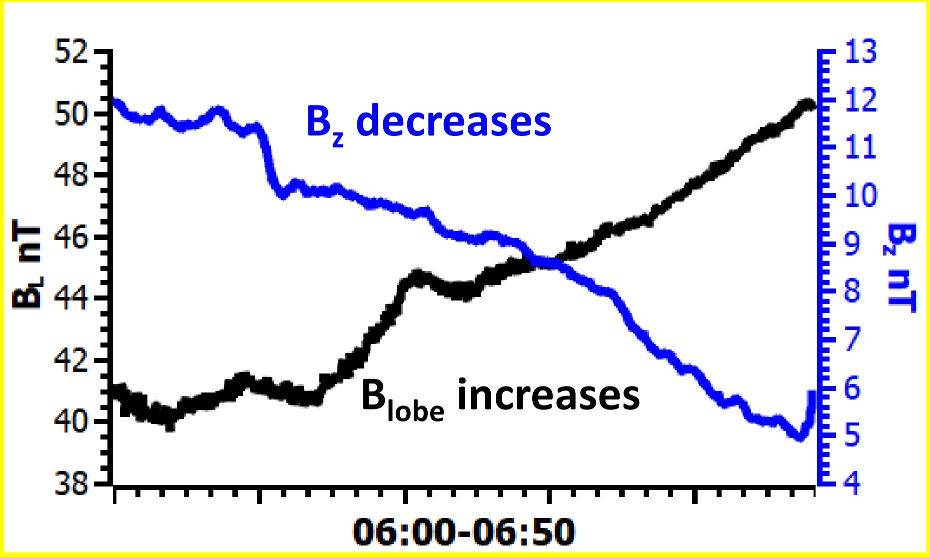

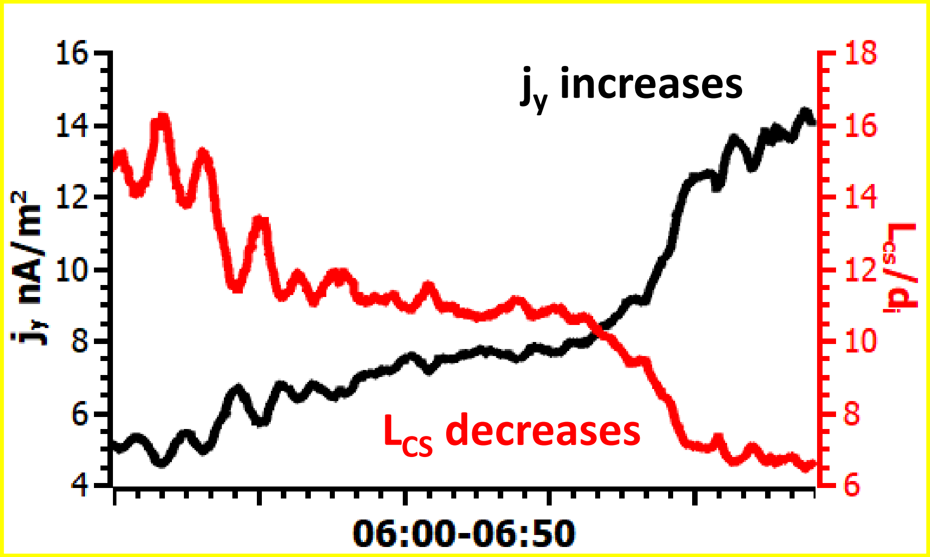

Current sheet dynamics: plasma cooling

An example of thinning CS observed by THEMIS; plasma data are collected around the equatorial plane

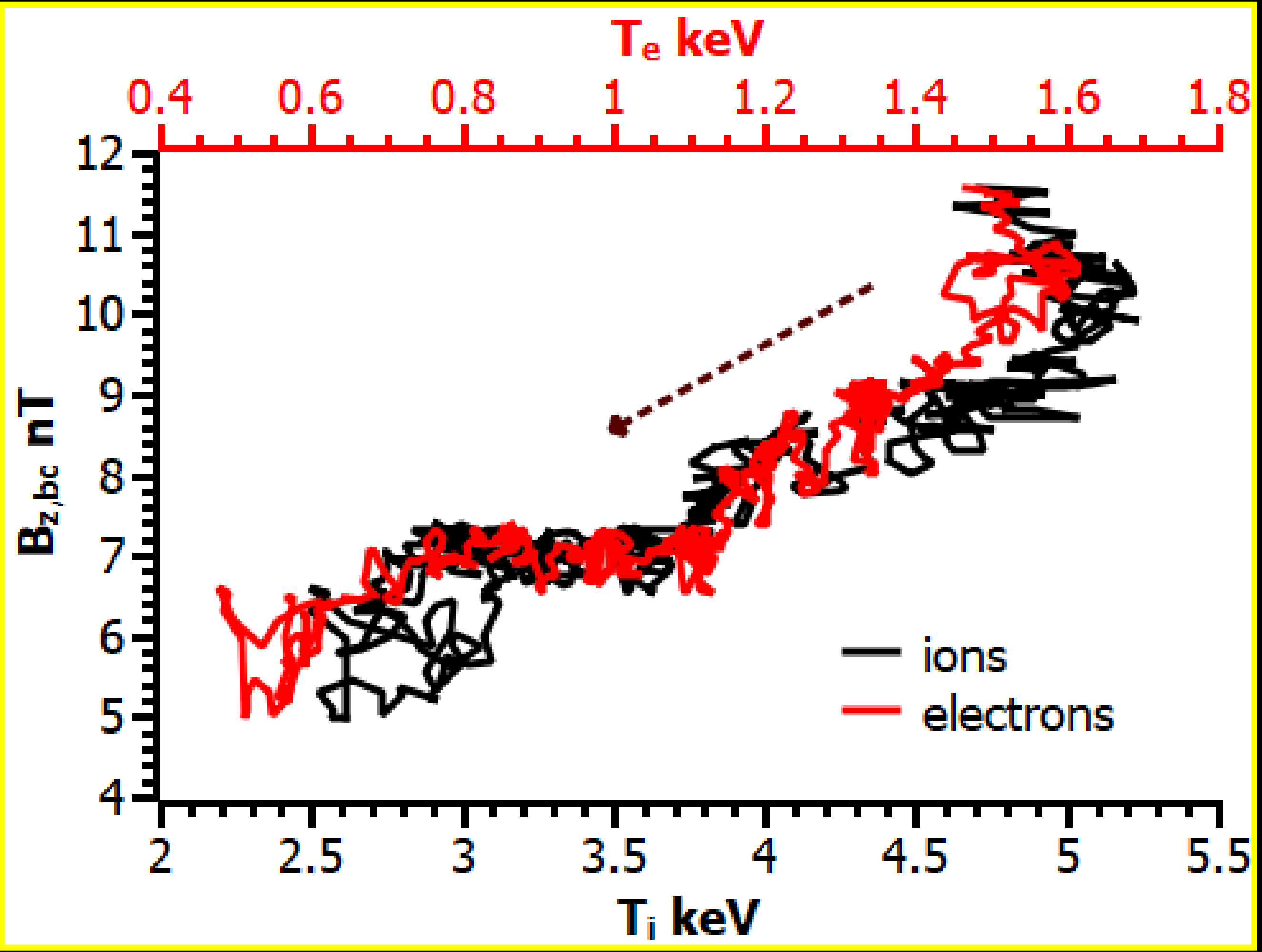

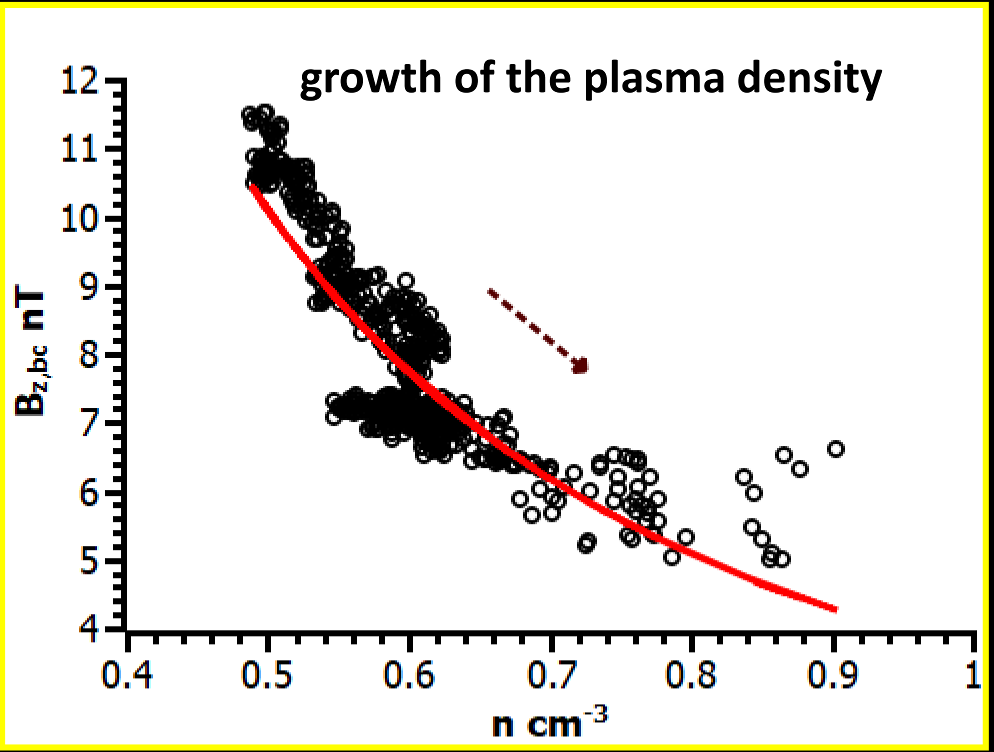

$$n_i \sim 1/B_z^{2/3}$$

$$T_{i,e} \sim B_z^{1/4}$$

+ Electrons are cooling faster than ions!

Current sheet dynamics: observations vs. model

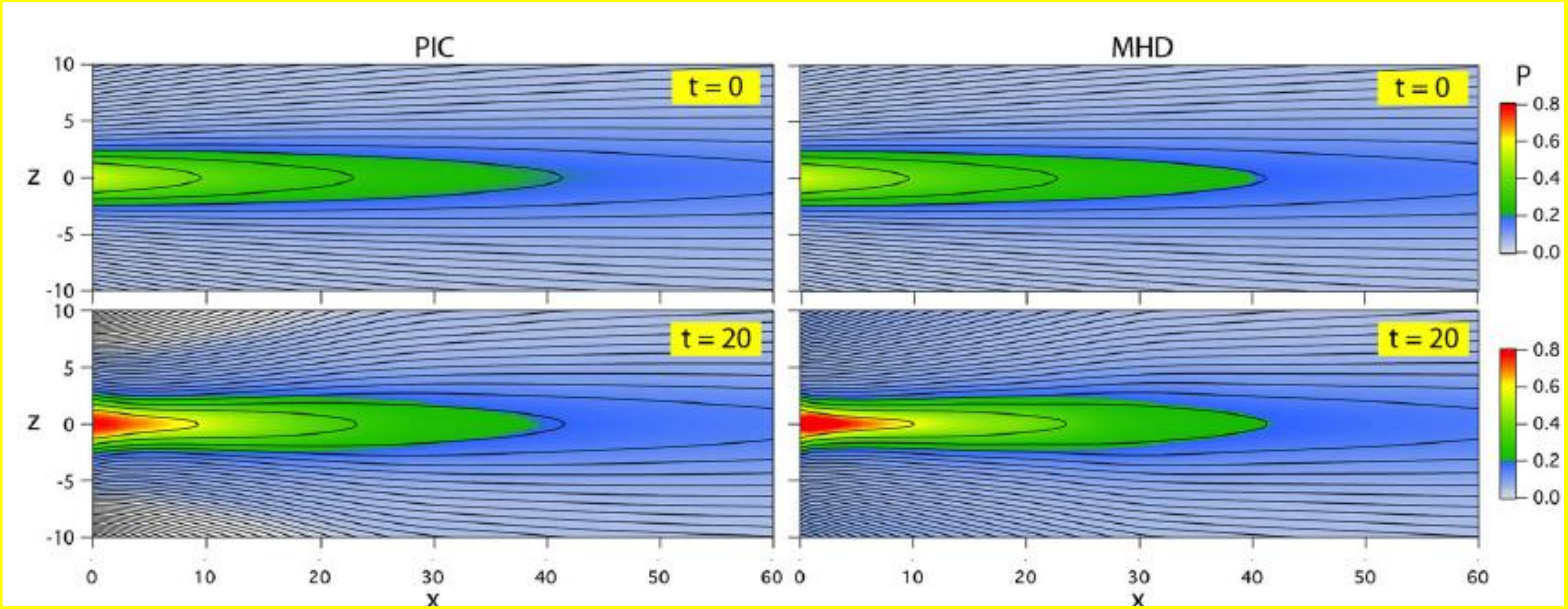

Birn & Hesse 2014

- Current sheet thinning is accompanied by (driven) pressure increase.
- Plasma entropy is conserved

$$pn^{-\gamma} \approx const$$

$$n \sim p^{3/5}, \quad T \sim p^{2/5}$$

Conclusions:

1. *CS embedding can be reproduced by simulations and analytical models*
2. *Temperature gradients well seen in observations, but are not included into kinetic simulations*
3. *Thin CSs are characterized by strong electron currents (both in observations and simulation)*
4. *Estimations suggest significant contribution of ion nongyrotropy (not yet observed!) and electron anisotropy to the pressure balance*
5. *Strong transverse electric fields are seen in simulations, but more accurate observations are required to estimate these field in the magnetotail*
6. *Models and observations of the electron anisotropy indicate on a finite field-aligned field in the magnetotail (not yet observed!).*
7. *CS thinning is accompanied by plasma cooling, but this effect is not seen in simulations.*

EARTH MAGNETOTAIL CURRENT SHEET

$$\nabla \times \mathbf{B} = \frac{4\pi}{c} \sum_{\pm} \int q_{\pm} \boldsymbol{v} f_{\pm} d\boldsymbol{v}$$

$$\nabla \cdot \mathbf{E} = 4\pi \sum_{\pm} \int q_{\pm} f_{\pm} d\boldsymbol{v}$$

2017

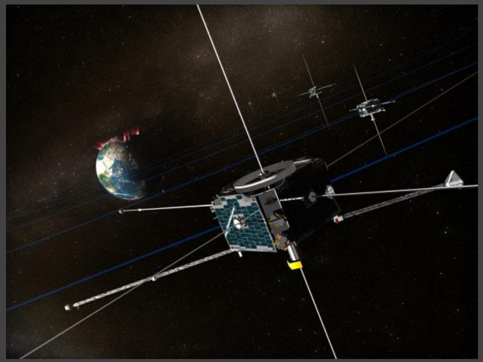

Predicted by models, but not yet observed

3

- $E_{\perp}$
- $E_{\parallel}$
- p_{xz}

Geotail, Cluster, THEMIS, ARTEMIS

4

Well observed, but not yet modeled

2

- ∇T
- $T\downarrow$

Additional info

Current sheet dynamics: current density growth

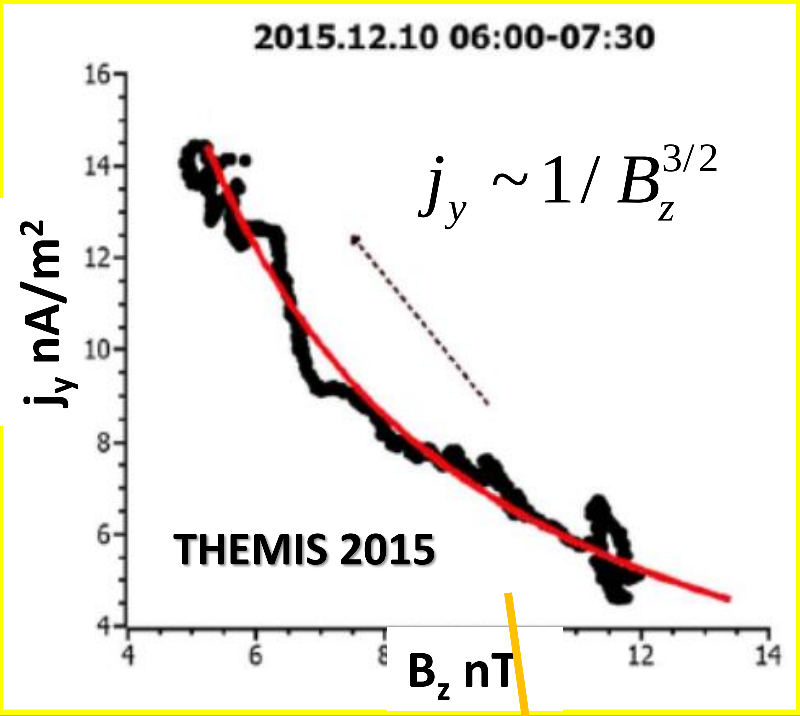

Artemyev et al., 2016

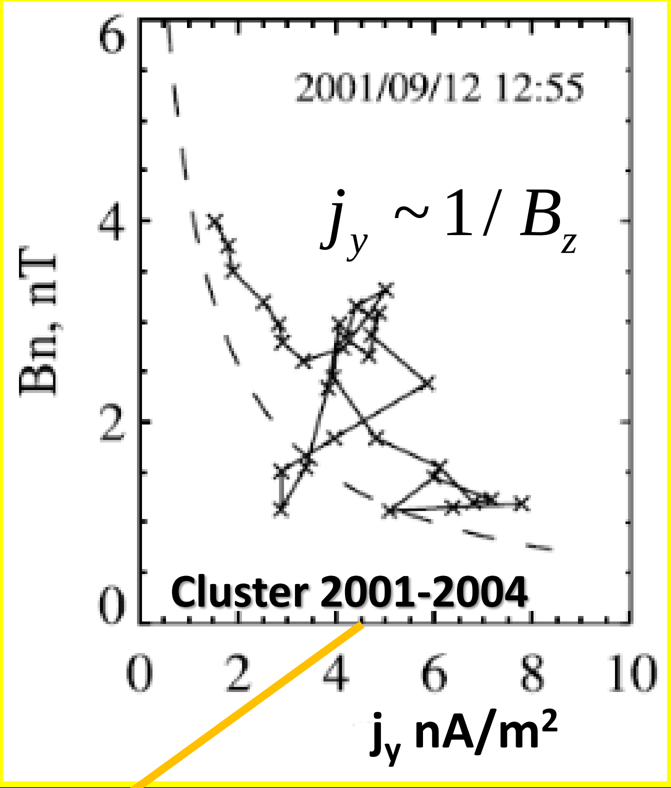

Petrukovich et al., 2007

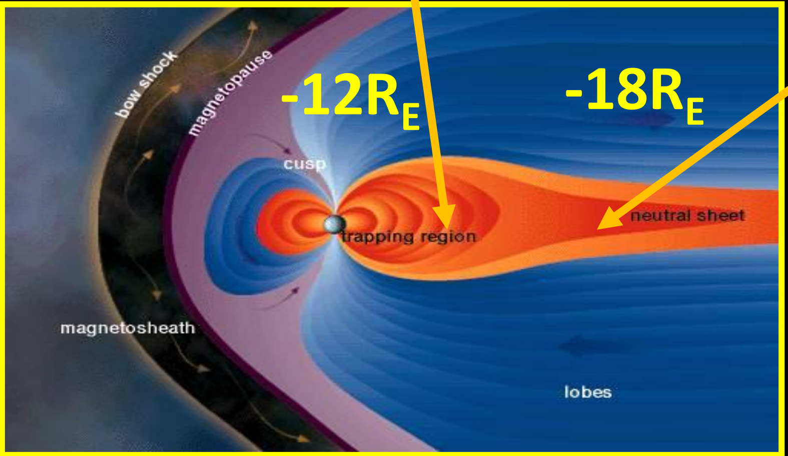

TCS properties:

- **CS thinning is not uniform process: larger initial B_z in the near-Earth CS requires more significant B_z decrease during thinning**
- **B_z is smaller at larger r, whereas j_y is larger at smaller r**

Petrukovich et al., 2013

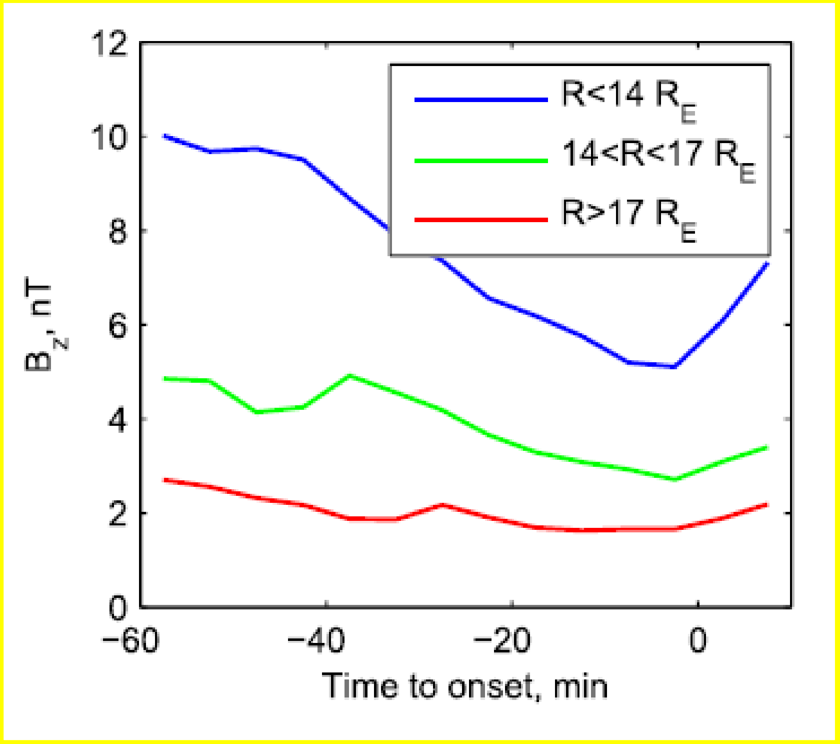

Formation of thin C

Thin current sheets and magnetotail dynamics

Karl Schindler
Fakultät für Physik und Astronomie, Ruhr-Universität Bochum, Germany

Joachim Birn
Los Alamos National Laboratory, Los Alamos, New Mexico

1999 JGR

$$p^{1/\gamma}V = N$$

Plasma pressure in the neutral plane

$$P^{1/\gamma}\int_{P}^{\hat{p}^*} \frac{\mathrm{d}\hat{p}}{|\mathrm{d}\hat{p}/\mathrm{dx}|\,[2\mu_0(\hat{p}-P)]^{1/2}} = N$$

$$p_0(x,t) = \frac{p^*(t)}{1+\Lambda(t)x}$$

γ=5/3

$$\hat{L}_{TCS} = \frac{B_0}{\mu_0|j_y(0,0)|} \propto \Lambda^{-2}p*^{2/\gamma-3/2}$$

$$J = \Lambda^2 p^{*2-2/\gamma}$$

This shows that the current density enhancement is more sensitive to a change in the x−gradient scale (Λ) than to an increase in lobe magnetic pressure (p^*).

The influence of magnetic flux depletion on the magnetotail and auroral morphology during the substorm growth phase

M.-S. Hsieh[1] and A. Otto[1]

2014 JGR

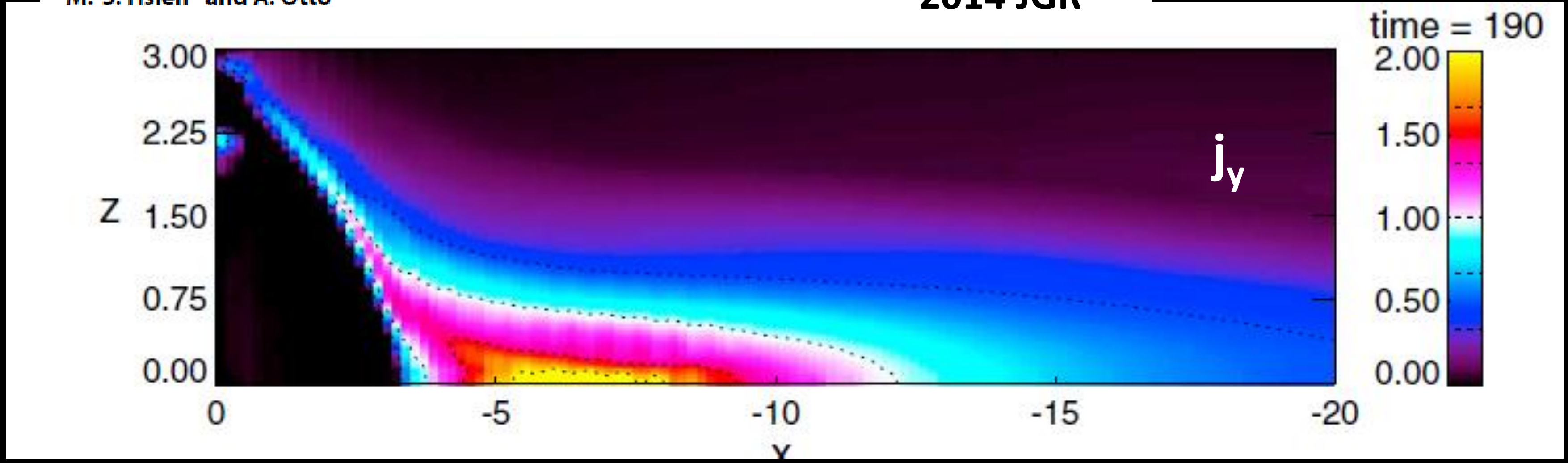

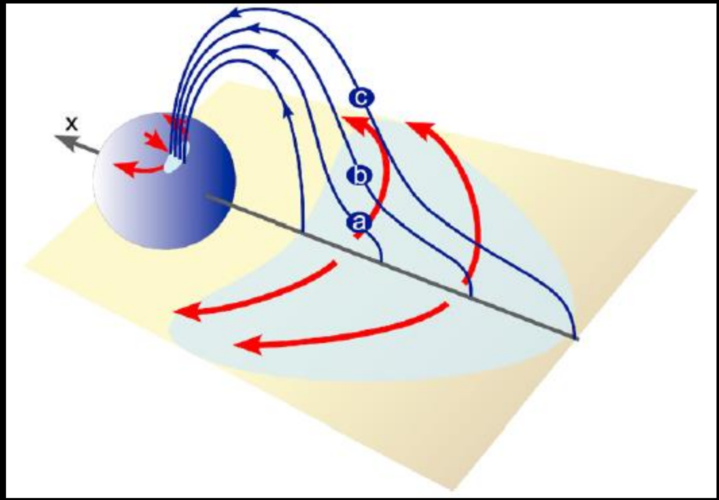

Modern CS models

2D solution with magnetic "hump"

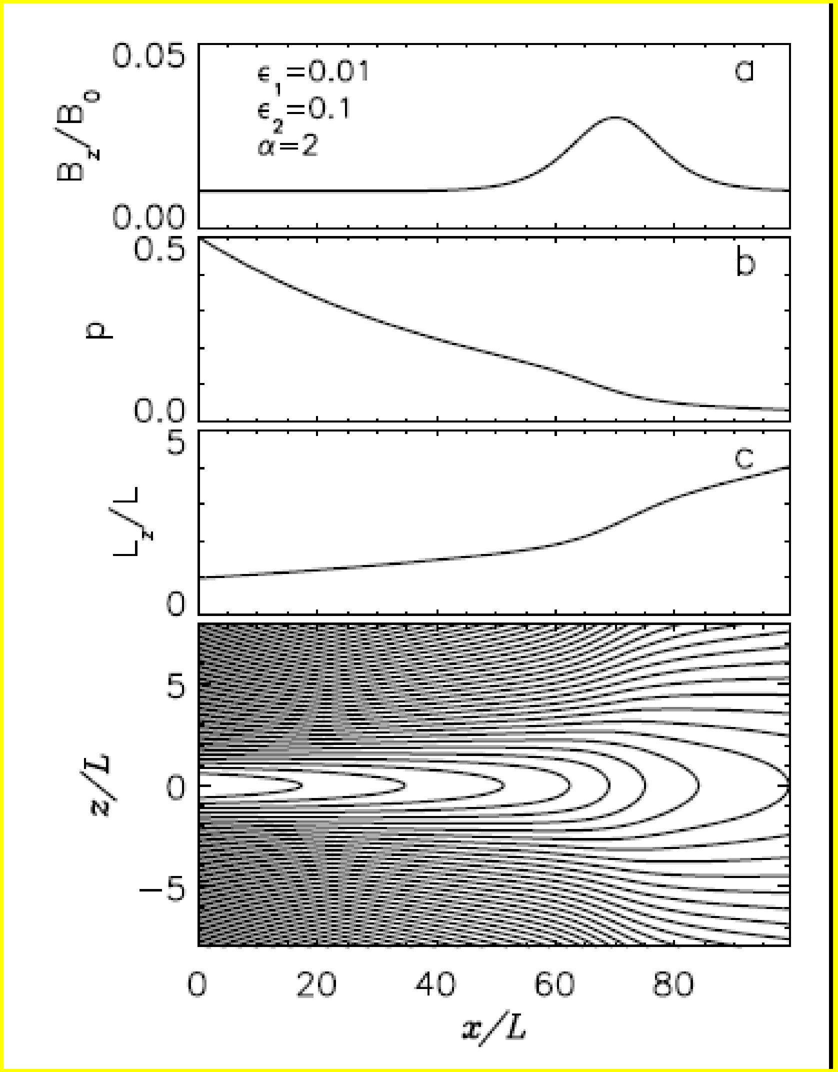

Sitnov & Schindler 2010

2D solution with small population of nongyrotropic ions

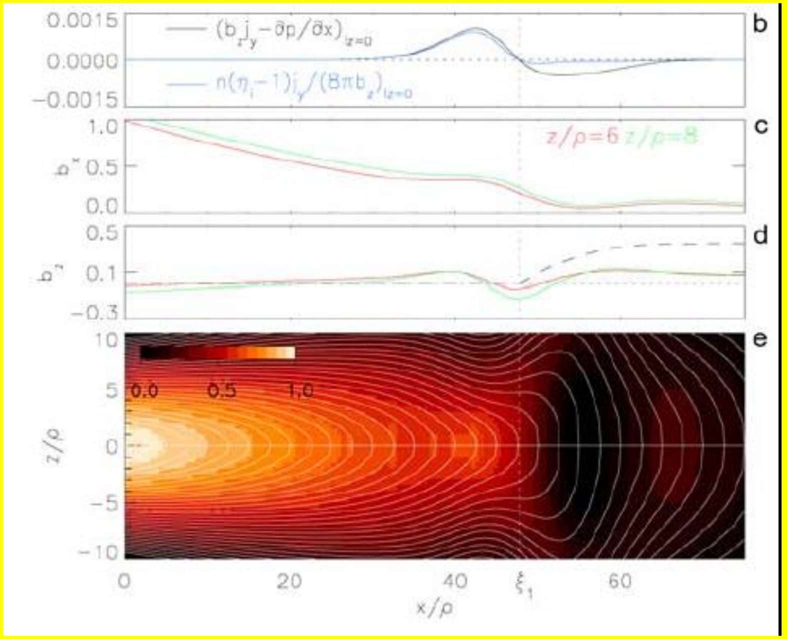

Sitnov et al., 2007

2D solution with included dipole!

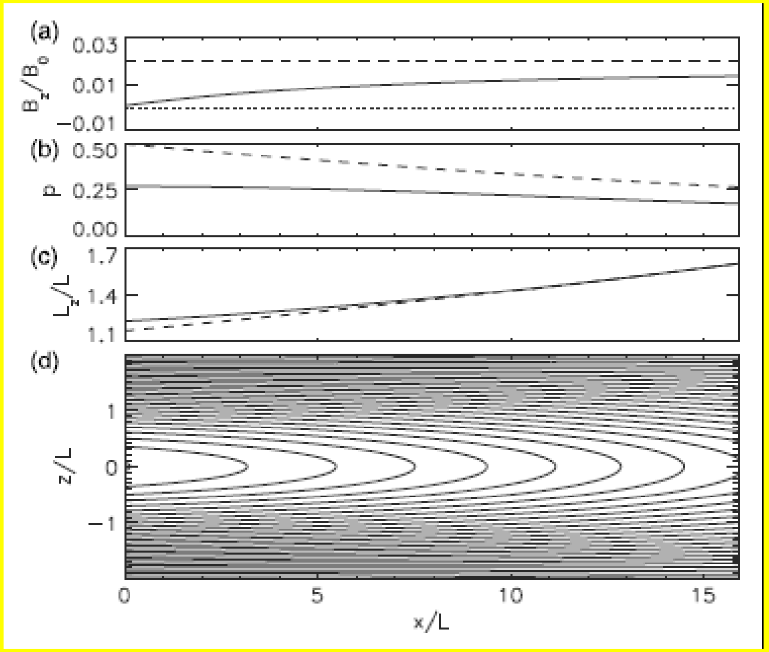

Sitnov & Merkin 2016

Recent reviews about CS structure & dynamics

- Artemyev, A. V., and L. M. Zelenyi (2013), Kinetic structure of current sheets in the Earth magnetotail, *Space Sci. Rev.*, *178*, 419–440, doi:10.1007/s11214-012-9954-5.
- Baumjohann, W., et al. (2007), Dynamics of thin current sheets: Cluster observations, *Ann. Geophys.*, *25*, 1365–1389.
- Birn. J, et al. (2012) Particle acceleration in the magnetotail and aurora *Space Sci. Rev.* **173** 49–102
- Eastwood, J. P., H. Hietala, G. Toth, T. D. Phan, and M. Fujimoto (2015), What controls the structure and dynamics of Earth's magnetosphere?, *Space Sci. Rev.*, *188*, 251–286, doi:10.1007/s11214-014-0050-x.
- Egedal, J., A. Le, and W. Daughton (2013), A review of pressure anisotropy caused by electron trapping in collisionless plasma, and its implications for magnetic reconnection, *Phys. Plasmas*, *20*(6), 061201, doi:10.1063/1.4811092.
- Ganushkina, N. Y., et al. (2015), Defining and resolving current systems in geospace, *Ann. Geophys.*, *33*, 1369–1402, doi:10.5194/angeo-33-1369-2015.
- Goldstein, M. L. et al. 2015 Multipoint observations of plasma phenomena made in space by cluster *J. Plasma Phys.* **81** 325810301
- Petrukovich, A. A., A. V. Artemyev, I. Y. Vasko, R. Nakamura, and L. M. Zelenyi (2015), Current sheets in the Earth magnetotail: Plasma and magnetic field structure with Cluster project observations, *Space Sci. Rev.*, *188*, 311–337, doi:10.1007/s11214-014-0126-7.
- Schindler, K. (2006), *Physics of Space Plasma Activity*, 522 pp., Cambridge Univ. Press, Cambridge.
- Sitnov, M. I., and V. G. Merkin (2016), Generalized magnetotail equilibria: Effects of the dipole field, thin current sheets, and magnetic flux accumulation, *J. Geophys. Res. Space Physics*, *121*, 7664–7683, doi:10.1002/2016JA023001.
- Yoon, P. H. and Lui, A. T. Y., 2005 A class of exact two dimensional kinetic current sheet equilibria *J. Geophys. Res.* **110** A01202
- Zelenyi L M, Malova H V, Artemyev A V, Popov V Y and Petrukovich A A (2011) Thin current sheets in collisionless plasma: equilibrium structure, plasma instabilities, and particle acceleration *Plasma Phys. Rep.* **37** 118–60
- Zelenyi, L. M., A. I. Neishtadt, A. V. Artemyev, D. L. Vainchtein, and H. V. Malova (2013), Quasiadiabatic dynamics of charged particles in a space plasma, *Phys. Uspekhi*, *56*, 347–394, doi:10.3367/UFNe.0183.201304b.0365.